

Search for the Intermediate Boson, Lepton Pair  
Production, and a Study of Deeply Inelastic Reactions  
Utilizing High Energy Neutrino Interactions in Liquid Neon

C. BALTAY

Columbia University

R.B. PALMER, N.P. SAMIOS

Brookhaven National Laboratory

ABSTRACT

An experiment is proposed to utilize high energy neutrinos in order to search for: (a) the existence of the intermediate vector boson  $W_1$  as well as the scalar boson  $W_0$ , (b) the production of lepton pairs ( $\mu^-e^+$ ) and ( $\mu^-\mu^+$ ), and (c) to study the properties of the deeply inelastic reactions. An exposure of 900 K pictures in the NAL 15-ft cryogenic chamber filled with neon and containing an inserted plate should allow for: the detection of  $W_1$  if its mass is less than 14 GeV and  $W_0$  if its mass is less than  $\sim 6$  GeV,  $\approx 150$  lepton pair events and innumerable inelastic events with muon identification and  $\nu$  energy measurement. An additional exposure of 100,000 pictures in hydrogen with a double plate should serve to both normalize the  $\nu$  flux and complement the deep inelastic study in neon.

## I. GENERAL DISCUSSION

We propose to study the interactions of high energy neutrinos for the following purposes: (1) detection of possible production of the intermediate vector boson  $W_1$  and/or the scalar boson  $W_0$ , (2) measurement of the rate for  $(\mu^-e^+)$  and  $(\mu^-\mu^+)$  lepton pair production, and (3) general study of deeply inelastic reactions. The method involves utilizing the NAL 15-ft cryogenic chamber and the broad band neutrino beam with most of the exposure run at the highest possible accelerator energy and intensity. The chamber should be filled with neon for 900,000 pictures with an inserted thick plate for muon detection. An additional exposure of 100,000 pictures with the chamber filled with hydrogen and containing the aforementioned plate as well as a thin (1 1/2 radiation length) plate for  $\gamma$  detection is also requested. This latter run will serve as a  $\nu$  flux normalization as well as augment the deep inelastic study by providing for the identification of the hadronic component of these reactions. We would like to have 250,000 of the neon pictures at the earliest time possible, even if for some reason the plate can not be inserted in the chamber for such an early run. As will be discussed later in the section on muon identification, a chamber full of neon without a plate provides sufficient muon selection to make such an early run worthwhile.

The justification of the proposed investigation need hardly be repeated here since discussions of the

above have appeared at length in the literature. Suffice it to say that the W search will be extended by a large factor in mass (the present upper limit is  $\sim 2$  BeV), with good sensitivity to all of its possible decay modes; the search for the scalar boson, whose decay into lepton pairs is inhibited, is unique to this experiment; any measurement of the four fermion lepton pair production process has enormous impact on the basic understanding of the structure of the weak interactions; and finally, the deep inelastic region probes the nucleon at very small distances and thus provides sensitive tests of the dynamical models of the structure of the nucleon.

We will now discuss each of these physics objectives with respect to the above noted means of detection. The chamber filled with neon, which has a 24 cm radiation length and 79 cm interaction length, allows for both  $\mu$  and electron identification. The addition of an 85 cm (5 interaction length) stainless steel plate further improves the muon identification by an order of magnitude. Thus, both leptonic decay modes of the  $W_1$  are clearly identifiable. In addition, the neon chamber is the best, and probably the only tool to detect the possible hadronic decay modes of the  $W_1$  which are probably significant, and could be dominant, at large W masses. As such this exploration complements the spark chamber search for the  $W_1$  with respect to the  $\mu$  decay mode and expands it with respect to its possible decay into  $e\nu$  and hadron states such as multiple pions. The strength of this visual technique is further illustrated in the case of the possible scalar boson

$W_0$ . The scalar boson decay into lepton pairs is inhibited by helicity conservation; sensitivity to its hadronic decay modes is thus crucial. Furthermore, if both a vector and a scalar boson exist, and the vector boson is heavier, then its dominant decay mode is expected to be  $W_1^+ \rightarrow W_0^+ + \gamma$ , which would make the search for the vector meson via its leptonic decay modes more difficult. The existence of such a particle has been recently discussed, pointing out the rather plausible decay scheme  $W_1^+ \rightarrow W_0^+ + \gamma$ ;  $W_0^+ \rightarrow K^0 \pi^+$  where the  $W^+$  is produced via the standard reaction  $\nu + N \rightarrow N + \mu^- + W_1^+$ . Such a sequence is ideally suited to this proposed experiment in that the  $\mu^-$  is clearly identified; the  $\gamma$  ray converts and the decay  $K^0 \rightarrow \pi^+ \pi^-$  would be clearly visible and detectable in the chamber. One notes that this conjecture appeared after the first presentation of this proposal and, in our opinion, represents one of the multitude of surprising and exciting new physical phenomena that may occur and be detectable in this type of experiment. In this experiment, we would observe an intermediate vector boson  $W_1$  with mass up to 14 GeV (accelerator run at 500 GeV) or up to 12 GeV (accelerator run at 350 GeV) and a scalar boson with mass approximately half of the above values.

The measurement of lepton pair production,  $\nu_\mu \rightarrow \mu^- \mu^+ \nu_\mu$  and  $\nu_\mu \rightarrow \mu^- e^+ \nu_e$  in the coulomb field of a nucleus, poses different problems. While the vector and scalar boson search is mainly one of exceeding the threshold whereupon their cross

sections increase enormously, the comparable lepton pair cross sections are expected to be small ( $\approx 10^{-42}$  cm<sup>2</sup>) and only increase relatively slowly with neutrino energy. As such, one requires maximum  $\nu$  flux and massive targets. The broad band  $\nu$  beam and a fiducial volume of 10 tons of neon serve this purpose. Since the reactions are coherent and go as  $Z^2$ , the use of neon ( $Z=10$ ) increases the rate considerably in comparison with hydrogen, and the ability to observe the charge multiplicity in the bubble chamber and reject events with more than two charged particles should greatly reduce the background. In addition, the precise angular measurements of the leptons and their positive identification make the background problem, manageable. We expect a total of 50  $\mu^- \mu^+$  events and 100  $\mu^- e^+$  events if their production rates are as predicted by the universal point interaction. There are some theoretical conjectures that the  $\mu^- \mu^+$  process could be greatly enhanced over the  $\mu^- e^+$  process; it would therefore be very useful to set an upper limit on the rate for the  $\mu^- \mu^+$  process even if its actual detection proves to be too difficult. It should be pointed out that the sensitivity to both  $\mu^- \mu^+$  and  $\mu^- e^+$  pairs could turn out to be crucial since the  $W$  is expected to decay equally into  $\mu \nu$  and  $e \nu$ , while a breakdown of universality would lead to differences between  $\mu^- \mu^+$  and  $\mu^- e^+$  rates. Again, this experiment complements the search for those reactions to be undertaken by other experiments; furthermore, the importance of the physics results as well as the different systematic difficulties in these two approaches certainly calls for more than one endeavor.

The electron scattering studies as well as early  $\nu$  explorations have indicated the importance of studying the deeply inelastic reactions. This involves the total cross section measurement as well as detailed studies of the  $q^2$  (momentum transfer) and  $\nu = (E_\nu - E_\mu)$  lepton energy loss distribution at nearly all energies. Difficulties associated with detecting  $\sigma_t$  involve both the lack of knowledge of the  $\nu$  energy and the  $\nu$  flux. The former can be achieved by either utilizing a "monochromatic beam" or by detecting all the reaction products and thereby obtaining the neutrino energy via energy conservation. The monochromatic approach suffers in that it is not very monochromatic; it provides a 10% knowledge of  $E_\nu$ , at the cost of an enormously reduced rate of events (more than an order of magnitude). One can achieve similar  $\nu$  energy resolution with neon and still retain large event rates. The flux difficulty is common to all experiments and can be attacked via detailed knowledge of the  $\pi$  and K production spectra with subsequent calculation of  $\nu$  flux, or via the measurement of reactions with "known" cross sections such as the elastic in deuterium,  $N^*$  production in hydrogen, or some subset of the inelastic events themselves in neon. Again, this experiment complements other endeavors with comparable accuracy but different systematic difficulties.

The study of the deeply inelastic reactions involves investigation of  $q^2$ ,  $\nu$  distributions which depend only on the leptonic, as well as other parameters that depend on the hadronic components. Needless to say, the identification of

the muon is of crucial importance and is non-trivial in these higher multiplicity events. As noted above, the  $\nu$  energy is derived from a measurement of the total final state energy with an estimated accuracy of 10%, using in essence the neon as a high resolution calorimeter. This, in combination with the measurement of the muon angle and momentum allows a determination of  $q^2$  and  $\nu$  to similar accuracy. The nuclear effects arising from interactions in neon certainly complicate the analysis of details of the hadronic component; however, their effect should be very small on the leptonic parameters  $q^2$  and  $\nu$  at all but very small  $q^2$ .

The proposed hydrogen exposure of 100,000 pictures in the same broadband beam serves to normalize the  $\nu$  flux and to augment the deep inelastic study. The insertion of the thick plate for muon identification is essential in this study. A thin plate,  $1\frac{1}{2}$  radiation length thick, mounted 20 cm in front of the thick plate, affords  $\pi^0$  energy determination and thereby gives the neutrino energy to  $\pm 10\%$ . Thus with the knowledge of the  $\nu$  flux, one can measure the total cross section and the  $q^2$  and  $\nu$  distributions of the inelastic events on free protons. Comparing these distributions with those on neon (50% neutrons, 50% protons) allows us to extract neutron-proton differences.

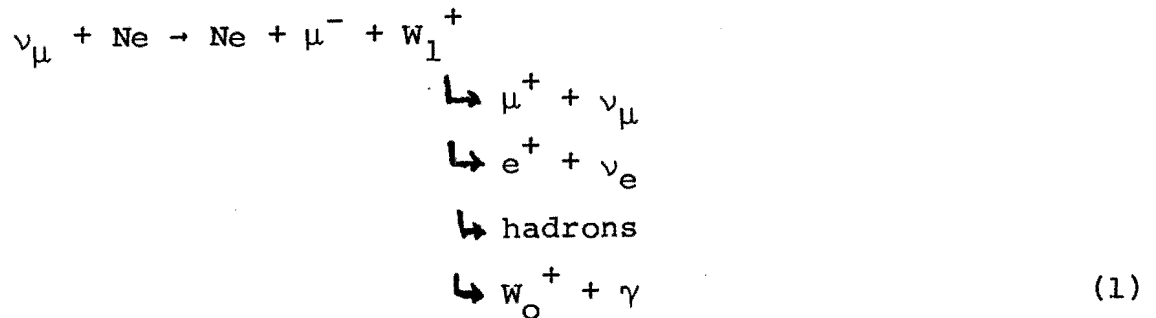
Since in this case the target is free protons, one is now in a position to study the details of the hadronic component of these inelastic reactions unhampered by nuclear effects encountered in neon.

Finally, a measurement of the  $N^*$  production on hydrogen, where the cross section is constant with a magnitude which should be well known, will serve to calibrate the absolute neutrino flux as well as its energy dependence. Therefore this exposure should be conducted under the same beam conditions as the neon run.

## II. DETAILED DESCRIPTION OF THE EXPERIMENT IN NEON

### A. Event Rates

The relevant reactions for this study are the W production processes



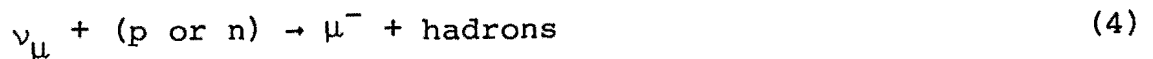
where  $W_1^{+}$  is the hypothetical intermediate vector boson and  $W_0^{+}$  is the recently proposed<sup>1</sup> scalar boson.

The four fermion processes are



where the coherent production dominates.

The inelastic reaction can be written as



where p or n indicate a proton or neutron in the neon nucleus.



In estimating the yield, we have used the calculation by Brown and Smith<sup>2</sup> for the W production, process (1), which includes both coherent and incoherent contributions. These cross sections are shown in Figs. 1 and 2. The cross section for the direct production of the scalar boson via reaction (2) is a function of both the scalar and the vector boson masses. These cross sections,<sup>3</sup> which include coherent and incoherent processes on neon, for several possible masses are shown in Fig. 2. They are typically a factor of 30 smaller than the vector boson cross sections. For the four fermion processes (3), we have used the cross section calculation by Czyz, Sheppy, and Walecka,<sup>4</sup> taking only the coherent part of the cross section (see Fig. 1). For the total inelastic cross section, we have assumed a linear dependence of the cross section on the neutrino energy, as found in the CERN  $\nu$  experiments,  $\sigma = 0.8 \times 10^{-38} E_\nu \text{ cm}^2$ , with  $E_\nu$  in BeV. The experimental evidence for the linear energy dependence is not very strong, and either the existence of the W or a breakdown of scale invariance could damp the total cross section significantly. Thus, the total number of inelastic events we calculate may well be an overestimate.

In calculating event rates, we have used the  $\nu$  fluxes calculated by F.A. Nezzrick et al<sup>5</sup> for the wide band, basic focused  $\nu$  beam. The decay length and the earth shield have been fixed at 400 m and 1000 m respectively. The  $\nu$  flux has been averaged over the area of the bubble chamber fiducial volume, 1.35 m radius. The flux curves for 200, 350, and 500 BeV primary accelerator energies are shown in Fig. 3.

We have used a fiducial volume of  $10 \text{ m}^3$  in front of the plate, and a density of 1.2 for the liquid neon. The event rate for a chamber filled with neon without a plate would be comparable since one must restrict the fiducial volume in this case also to allow room for muon identification. The numbers of events for a  $10^6$  picture run with  $2 \times 10^{13}$  protons on the target, and an effective one interaction length target, are shown in Table I. The number of vector and scalar bosons produced as a function of their masses is shown in Figs. 4 and 5. It is clear from the table and these figures that there is an overwhelming advantage to running at the highest accelerator energy possible. The distribution of the four fermion events and the total inelastic events in the incident  $\nu$  energy is shown in Figs. 6 and 7.

B. Identification and Analysis of Events and  
Discussion of the Backgrounds

1. The Process  $\nu_{\mu} + \text{Ne} \rightarrow \text{Ne} + \mu^{-} + \mu^{+} + \nu$

These expected 50 muon pair events have to be distinguished from  $\sim 6 \times 10^6$  neutrino interactions that will occur in the same exposure (assuming a total  $\nu$  cross section of  $0.8 \times E_{\nu} \times 10^{-38} \text{ cm}^2/\text{nucleon}$ ). The topology of the muon pair events is two outgoing charged prongs with no incident charged tracks (the recoil nucleus Z will be invisible if the leptons scatter coherently on the whole nucleus). The background events with two charged tracks in the final state will contain a  $\mu^{-}$  with a p or  $\pi^{+}$  from the reactions

$$\nu_{\mu} + n \rightarrow \mu^{-} + p \quad (5)$$

$$\rightarrow \mu^{-} + p + \pi^{0} \quad (6)$$

$$\rightarrow \mu^{-} + n + \pi^{+} \quad (7)$$

$$\nu_{\mu} + p \rightarrow \mu^{-} + p + \pi^{+} \text{ (p invisible)} \quad (8)$$

The  $\mu^{+}$  can be distinguished from a p or  $\pi^{+}$  by inserting a thick plate ( $\sim 6$  interaction length) in the path of the particle, and requiring that the particle pass through the plate without interacting. A detailed discussion of the muon identifier is given in Sec. V.

This signature can unfortunately be faked by a  $\pi^{+}$  which decays into a  $\mu^{+}$  before reaching the lead plate. The probability of a  $\pi^{+}$  decaying in a given distance  $d\ell$  in the liquid is

$$dN = -1/\lambda \, d\ell$$

where  $\lambda = p/m \tau_0 c$ . The  $\pi^{+}$  can also interact in the neon before reaching the lead plate; the probability of interacting in a given distance  $d\ell$  is

$$dN = -1/L \, d\ell$$

where  $L \approx 79$  cm, the interaction length in liquid neon. Then the fraction of pions which will decay in the neon before interacting is approximately  $L/\lambda$  (as long as  $\lambda \gg L$ ). This fraction, as a function of the pion momentum, is shown in Fig. 16. For a 2 GeV/c  $\pi^{+}$ ,  $\lambda \approx 110$  m; thus  $0.80/110 \approx 3/4\%$  of the  $\pi^{+}$  will decay and fake a  $\mu^{+}$ . Thus the most serious background is reaction (7) with a  $\pi$  decay. (The cross section for reaction (8) is  $\sim 3$  times that of reaction (7) but the proton will usually be visible, reducing the background due to (8) to a small fraction of that due to (7).)

The cross section for reaction (7) is expected to be<sup>6</sup>

$$\sigma(\nu_{\mu}n \rightarrow \mu^{-}n\pi^{+}) \approx 0.24 \times 10^{-38} \text{ cm}^2/\text{nucleon}$$

independently of  $E_{\nu}$ . We calculate the expected number of events due to this reaction to be 32,000 at 500 BeV, less at lower primary proton energies. Making some reasonable assumptions about the  $\pi^{+}$  momentum spectrum in these events, we made a rough estimate of the number of these events which will fake a muon pair due to  $\pi$  decay. Their total number is  $\sim 240$ .

The number of these background events may be further reduced in the following ways:

a. The decay angle in the  $\pi^{+} \rightarrow \mu^{+}$  decays will probably be too small ( $\sim 5$  to  $30$  mrad) to be detected with confidence in liquid neon. However, there will be a substantial momentum change in the decay (the  $\mu^{+}$  momentum will be evenly distributed between  $\sim 1/2$  and  $1$  times the  $\pi^{+}$  momentum). Since there should be on the order of  $1/2$  m of  $\pi^{+}$  track on the average before decay, the momentum change can be used to confidently eliminate roughly half of the background events with  $\pi^{+} \rightarrow \mu^{+}$  decays.

b. The angular and momentum distributions of the  $\pi^{+}$  from the reaction  $\nu + n \rightarrow \mu^{-} + \pi^{+} + n$  from the CERN heavy liquid bubble chamber  $\nu$  experiment are shown in Fig. 8. These  $\pi^{+}$ 's are relatively slow and their angular distribution is quite broad. (95% of the  $\pi^{+}$  have lab angles over  $10^{\circ}$ .) Loveseth and Radomski<sup>7</sup> have pointed out that the transverse momentum distribution of the  $\mu^{+}$  in the lepton pair events may not be very different from that of the background events. A

selection on the lab angle of the  $\mu^+$  can however, be used to select the lepton pair events. The angular distribution of the  $\mu$ 's from the coherently produced  $\mu^+\mu^-$  pairs have been calculated by Fujikawa;<sup>6</sup> they are extremely sharply forward peaked, nearly all  $\mu^+$  being within  $2\ 1/2^\circ$ , as shown in Fig. 9. A cut on the laboratory production angle of the  $\mu^+$  will reduce the  $\mu^+$  from  $\pi^+$  decay background by a very large amount, while losing very few of the  $\mu^+\mu^-$  pair events. However, since the CERN events shown in Fig. 8 were produced by  $\nu$ 's of much lower energy than the ones considered here, we assume only a factor of 30 in background reduction due to kinematic selections.

The above considerations will reduce the background to  $240 \times 1/2 \times 1/30 \sim 4$  events

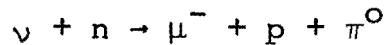
to be compared with the expected signal of 50 muon pair events.

These remaining background events are a subset of a parent sample of  $\sim 32,000 \nu n \rightarrow \mu^- n \pi^+$  events. A study of this large parent sample should make it possible to estimate the number of background events and to do a background subtraction, with a systematic uncertainty of possibly some fraction of the size of the background.

2. The Process  $\nu_\mu + \text{Ne} \rightarrow \text{Ne} + \mu^- + e^+ + \nu_e$

The characteristic appearance of these events, reaction (3), in the bubble chamber will be a vertex with two charged prongs; the negative being a  $\mu^-$  which is identified by the fact that the track passes through the  $\sim 6$  interaction length plate without interacting; the positron will be unambiguously identified by its characteristic appearance in liquid

neon (radiation length  $\sim 24$  cm). The main, and probably the only, background will be due to reaction (6)



when a) the proton is too slow to be visible, b) the  $\pi^0$  produces a Dalitz pair which is so asymmetric that the  $e^-$  is undetectable.

The cross section for reaction (6) is expected to be<sup>8</sup>  
 $\sigma(\nu n \rightarrow \mu^- p \pi^0) \approx 0.32 \times 10^{-38} \text{ cm}^2/\text{nucleon}$ . We thus expect a total of  $\sim 45,000$  events of reaction (6) to be produced in the experiment. Of these,  $\sim 1/30$  will have an invisible proton (this number is based on the CERN results). Only  $1/80$  of these will produce a Dalitz pair, and much less than 1% of these will be sufficiently asymmetric to look like a single positron. This produced a background of

$$(45,000 \times 1/30 \times 1/80 \times 1/100) < 1$$

or less than one event, compared to the expected  $100 \mu^- e^+$  events.

The  $\mu^- e^+$  pairs should thus be very clean.

### 3. Leptonic Decays of the W

The W production and decay into  $\mu^+ \nu$  and  $e^+ \nu$  will look very similar to the lepton pair production reactions (3a) and (3b). The  $e^+ \nu$  events should be very clean, as discussed above. For the  $\mu^+ \nu$  decays, the main background is the 240 events of reaction (7), followed by  $\pi^+ \rightarrow \mu^+ \nu$  decay, as discussed above. The kinematic distinction in the case of the W decay is however based on the transverse momentum distribution of the  $\mu^+$ . The  $\pi^+$  from reaction (7) is expected to fall off as  $e^{-P_{\perp}/0.3}$  as deduced from the CERN data. The transverse momentum distribution of the  $\mu^+$  from W decay

will be very large, peaking near  $1/2 m_W$ . The expected distribution for the background and 10 BeV W decays are shown in Fig. 10. A cut at  $P_{\text{trans}} \cong 1$  BeV will reduce the background by a factor of  $\sim 1/30$ , to  $\sim 8$  events, while losing only 6% of the W events. As the W mass gets higher, the kinematics become even more favorable. A signal of 100 W decays should thus be quite convincing.

#### 4. Hadronic Decays of the W

A very massive vector boson will probably have substantial, and possibly dominant, hadronic decay modes. A scalar boson cannot decay into a lepton pair, and is thus expected to have dominant hadronic decays. In a neon chamber, we can measure the momenta and angles of the charged hadronic decay products, detect and reconstruct neutral hadrons decaying into  $\gamma$ 's, with high efficiency (radiation length  $\sim 24$  cm), see  $K_S^0$  decays, and possibly even detect a large fraction of the neutrons by their interactions (collision length  $\sim 79$  cm). We can thus calculate the effective mass of any combination of hadrons produced along with a  $\mu^-$ ; the W should manifest itself as a peak in the effective mass distribution at the mass of the W. The large background of inelastic events can be eliminated to a very large extent by making use of the very different distribution of these events in  $q^2$  and  $\nu$ . The inelastic events are expected to be distributed over a large range of these variables, while the W events will be concentrated at very small  $q^2$  and large  $\nu$ . Selecting the region where the W's are concentrated should reduce the

inelastic background by a factor 100 or so. These remaining events will be spread out over a large range of hadron effective mass, and a W peak of 100 events should be easily recognizable. A neon bubble chamber is the best, and probably the only way to identify individual hadronic decay modes and branching ratios.

5. The Decay  $W_1^+ \rightarrow W_0^+ + \gamma$

If both a vector and a scalar boson,  $W_1^+$  and  $W_0^+$ , exist, and the vector boson is heavier, then the dominant decay of the vector boson would be into a scalar boson and a  $\gamma$ , followed by hadronic decay of the scalar boson. This would make the search for the vector boson via its leptonic decay modes very difficult. In a neon chamber, this decay can be detected since the  $\gamma$  will convert into  $e^+e^-$  pair with very high efficiency (radiation length in neon is  $\sim 24$  cm, average path length in chamber is  $\sim 1$  m). The hadronic decay products of the  $W_0$  can be detected, as discussed above, and the  $W_0 + \gamma$  effective mass can be then computed.

6. Analysis of the Inelastic Events

As is indicated in Table I, the inelastic events will, unless the intermediate boson mass is less than 5 GeV, form the vast majority of all events seen in the chamber. Their analysis can be divided into two parts: a) the study of their distribution in variable that depends only on the four momenta of the leptons ( $E_\nu, q^2, \nu$  as defined below), and b) the study of these reactions including variables which depends on the observation of the distribution of the hadrons.



In the first case, we require ideally to know the spectrum of neutrinos, the neutrino energy  $E$  for each event and the angle  $\theta$  and energy  $E'$  of the outgoing muon. The identification of which track is the muon is obviously crucial and to this end either the plate or a neon filling, or an external muon detector is essential. The estimation of the neutrino energy can be made in neon to about 10% up to neutrino energies of 200 GeV. The error at the higher momenta is dominated by measurement error on the fastest outgoing track, in general the muon. The error at lower momenta is more effected by the ability in neon to estimate the energy given to  $\pi^0$ 's. However, as will be discussed in more detail when we consider the hydrogen filling, the fraction of energy going to  $\pi^0$ 's is not likely to be large and thus an error of as much as 20% in the estimation of  $\pi^0$  energy is not likely to effect the error in  $E$  by more than 4%. The energy given to neutrons is expected to be small since at high energy the interaction will have a peripheral character (pomeron exchange is often discussed) and the nucleon should be left with a low momentum. Even if this were not the case, the high nuclear cross section in neon will allow the observation of fast neutrons in some cases and thereby establish a correction.

The second variable  $q^2$  is given by

$$q^2 = 2EE'(1-\cos\theta)$$

which for small angles  $\theta$  can be expressed approximately.

$$q = E'\theta \sqrt{\frac{E}{E'}}$$

$E'$  and  $\theta$  are the energy and angle of the observed and identified outgoing muon and both are determined with accuracy better than 10% up to neutrino energies of the order of 200 GeV. The dependence on the total neutrino energy is seen to be relatively weak.

The third variable  $\nu$  is equal to the difference in energy between the muon and neutrino and thus equal to the total hadronic energy. With the good  $\pi^0$  conversion efficiency in neon, we expect this to be determined to about 5% up to neutrino energies of 200 GeV.

We will thus be able to obtain the distribution of events in the variables  $E_\nu$ ,  $q^2$ , and  $\nu$ . Since the number of events is very large, we will be able to explore the dependence of the cross section on each of these variables in detail. The adequate statistics are necessary to separate the contributions to the cross section from the three structure functions  $W_1$ ,  $W_2$ , and  $W_3$  defined by

$$\frac{d^2\sigma}{dq^2 d\nu} = \frac{G^2}{2\pi} \left[ W_2 \cos^2 \frac{2\theta}{2} + 2W_1 \sin^2 \frac{2\theta}{2} + \frac{E+E'}{m} W_3 \sin^2 \frac{2\theta}{2} \right] .$$

$W_1$ ,  $W_2$  and  $W_3$  are each functions of  $q^2$  and  $\nu$ . If the  $\nu$  spectrum is known, then for all fixed values of  $q^2$  and  $\nu$ , the contributions of each of the three structure functions can be separated by their different energy dependences. If the spectrum is not known its shape can be deduced from the experimental distributions at all but very low energies (see Sec. IV). The structure functions can then be separated at all but the low values of  $q^2$  and  $\nu$ . Scale invariance can

be checked separately for  $W_1$ ,  $W_2$  and  $W_3$  and their values can be compared with the predictions of various models of nucleon structure. The importance of such a study is well known. Scale invariance implies pointlike behavior within the nucleon which can be probed to ever smaller distances by exploring at ever higher momentum transfers. In this experiment,  $q^2$  up to  $400 \text{ (GeV/c)}^2$  are accessible and details of the cross section at such momentum transfers will provide very sensitive tests of the different models.

### 7. W Search Using the Total Cross Section

Of particular interest in the study of the deep inelastic  $\nu$  interactions is the dependence of the total cross section  $\sigma_{\text{tot}}$  on  $E_\nu$ , the  $\nu$  energy. Assuming scale invariance and locality,  $\sigma_{\text{tot}}$  is expected to increase linearly with  $E_\nu$ . This prediction is modified by a factor of  $(1 - q^2/m_W^2)^{-2}$  if the  $W$  exists. This effect of the  $W$  on the total cross section is shown in Fig. 11. A measurement of the total cross section is thus a sensitive search for the intermediate boson with masses possibly up to 20 or 30 BeV. The total number of inelastic events in neon is shown in Fig.7; there are  $\sim 5000$  events/10 BeV bin all the way up to 300 BeV. The main problem in this search is thus systematic-mainly the knowledge of the  $\nu$  spectrum and the measurement of  $E_\nu$ . It is however possible to cancel out the uncertainties due to the  $\nu$  spectrum by looking at the energy dependence of the cross section at fixed  $q^2$  and  $\nu$ , since we have this information for all events. The curves of Fig. 11 are averaged over  $x$  and  $\nu$ ; at high  $x$  and  $\nu$

the sensitivity on the existence of heavy  $W$ 's is much greater. Of course, if the cross section turns over, it may either be due to the  $W$ , or breakdown of scale invariance; either possibility is of great interest. However, if  $\sigma_{\text{tot}}$  keeps rising linearly with  $E_{\nu}$  up to 300 BeV, it is a meaningful negative result.

### III. THE HYDROGEN RUN

We are requesting 100,000 pictures with the chamber filled with hydrogen with both the thick plate described above and also a thin (1-in. stainless steel) plate placed 20 cm in front of the thick plate (see Fig. 17). It would be important that the beam conditions should be the same in this and the neon run, since the object of this run is to allow some calibration of the neutrino spectrum and also to determine neutron proton differences in the inelastic interactions. The heavy plate will allow identification of the outgoing muon and the thin plate will allow a determination of the neutrino energy to  $\pm 10\%$ , by conversion of  $\gamma$  rays from  $\pi^0$ 's produced in the interactions.

The thick plate and its efficiency as a muon detector is discussed in Sec. V. The efficiency of the thin plate in aiding in the neutrino energy determination arises in part because on average only a fraction of the neutrino energy will go into  $\pi^0$ 's. From experience at CERN, we estimate that the energy from a given high energy inelastic event will be divided roughly as follows:

- 1/2 the initial energy to outgoing muon.
- 2/6 the initial energy to charged pions.
- 1/6 the initial energy to neutral pions.

Negligible fraction of the initial energy to nucleons. In any case, it is unlikely that a large fraction of the initial energy will be given to neutral pions. If then we can estimate this part of the energy to even a low accuracy like 20%, the resultant contribution to the total energy will be small. If as proposed here, a single 1 1/2 radiation length plate is inserted 20 cm in front of the thick plate, then 80% of all  $\gamma$  radiation will be converted in that plate. If the neutrino energy is 200 GeV, the mean  $\pi^0$  energy would be of the order of 40 GeV for one  $\pi^0$ . If the  $\gamma^0$ 's are converted, then four electrons of energy about 10 GeV each would be observed and each could be measured to about 40% (for  $\sim 4 \mu$  accuracy on film), or  $\pm 4$  GeV.

Since four measurements are involved, their contribution to the uncertainty in neutrino energy would be  $\sqrt{4 \times 4} = 8$  GeV or only 4% of the total neutrino energy. Another contribution of 4% would come from the failure of the plate to convert all  $\gamma$  rays. But the total error from determination of  $\pi^0$  energy would still be of the same order as that arising from errors in measurement of the fast muon ( $\sim 5\%$  for 2 m of track). Note that the measurement can be made through the plate, the coulomb scattering in the plate introducing an error of only 5%. We conclude therefore that the addition of the 1 in. plate will allow estimation of the neutrino energy to the order of 10% at energies of the order of 200 GeV. This is at least as good as that provided by monoenergetic beams up to this energy.

We will now consider the rates. The events of special interest here are:

$$\begin{aligned} \nu + p &\rightarrow \mu^- + N^{*++} \\ &\rightarrow p + \pi^+ \end{aligned} \quad (9)$$

and the inelastic interaction

$$\nu + p \rightarrow \mu^- + \text{hadrons} \quad (10)$$

A run of 100,000 pictures with  $2 \times 10^{13}$  protons on the target is assumed, with 67% target efficiency. The horn beam is assumed and the fiducial volume taken as  $10 \text{ m}^3$ . The number of events produced at various primary proton energies are:

	<u>200 BeV</u>	<u>350 BeV</u>	<u>500 BeV</u>
$N^*$ Production	550	900	1300
Inelastic	7000	16000	32000

This exposure, although small, would provide larger numbers of events than would be obtained with  $10^6$  pictures in a monoenergetic beam, with a knowledge of the neutrino energy as good at 200 GeV and better at lower energies. Since the experiment would be run under the same conditions as the neon run it would allow:

1. The calibration of the absolute neutrino flux given a knowledge of the  $N^*$  production cross section. Such knowledge should be available from runs in deuterium at BNL and Argonne as well as from propane runs at CERN.

2. Some knowledge of the shape of the neutrino spectrum assuming the flatness of the  $N^*$  cross section, which follows directly from locality and the existence of some reasonable form factors.

3. A determination of the total  $\nu p$  cross section, which with the neon run will allow a determination of the  $\sigma_{\nu n}/\sigma_{\nu p}$  ratio and other studies of the neutron proton differences which have great significance.

4. Allow a study of the details of the hadronic components of the inelastic interactions without the complications of secondary interactions in the neon nucleus and at the same time allow an estimation of these effects by comparing the results with those in the larger and statistically much better neon sample.

In conclusion, we would emphasize that the hydrogen run is requested as an ancillary to the neon exposure, to be analyzed along with that exposure. The use of the thick plate will mean that the muon detection in the two experiments will be similar. The use of the thin plate will provide adequate detection of  $\pi^0$ 's and again assure that the analyses are similar.

#### IV. DETERMINATION OF THE $\nu$ SPECTRUM

The spectrum can be determined either by calculations<sup>1</sup> from observations on the beam, including production distributions from the target, K to  $\pi$  ratios, observations of distributions in the decay tunnel and observation of the

distribution of muons in the shield; or 2) from observation on the distribution of events in the chamber. In the first category, the best would appear to be the observation of the separate distribution of pions and kaons in the decay tunnel by the use of the bubble chamber charged particle beam and its proposed Cerenkov detectors. To this end, we request 1. that a magnet be placed in the target area at the end of the decay region such that particles passing through the hole in the beginning of the shield are deflected down the charged particle beam. This magnet should be capable of deflecting momenta up to a minimum of 200 GeV. 2. A magnet be placed immediately after the horn system such that particles produced at different angles can be deflected into the hole. The magnet should be able to deflect 200 GeV through at least 1 mrad.

The second means of determining the spectrum depends on the observation of known cross sections or cross sections whose energy dependence is known. In deuterium, the elastic cross section ( $\nu+n \rightarrow \mu^-+p$ ) at small  $q^2$  is known from  $\mu$  decay and can provide an absolute calibration of the flux in such an exposure. In the same exposure  $N^{*++}$  ( $\nu+p \rightarrow \mu^-+p+\pi^+$ ) production can be observed and thus its cross section accurately established. This will be done at both BNL and Argonne. The observation of  $N^*$  production on hydrogen can thus be used to calibrate spectra at NAL. This then is one reason why we prepare a short run with hydrogen under identical beam conditions. The proposed run will allow determination of the absolute rate of  $N^*$  production to better than 5% and thus normalize the absolute flux to approximately this accuracy.



The detailed shape of the neutrino spectrum can then be determined with minimal assumptions, from the inelastic events themselves.

Assuming only the locality of the weak interaction at the current hadron vertex we can write

$$\frac{d\sigma}{dq^2 d\nu} = \frac{q^2}{2\pi} \frac{E'}{E} \left[ W_2 \cos^2 \frac{\theta}{2} + 2W_1 \sin^2 \frac{\theta}{2} + \frac{E+E'}{M} W_3 \sin^2 \frac{\theta}{2} \right] .$$

For events with small  $\nu$  and  $q^2$  then

$$\frac{d\sigma}{dq^2 d\nu} \approx \frac{q^2}{2\pi} \left[ W_2 + \frac{q^2}{2E_m} W_3 + \frac{q^2}{2E^2} W_1 \right] .$$

$W_1/W_2$  and  $W_3/W_2$  are bounded and so we note that for fixed  $\nu$  and  $q^2$  and  $E > q^2/2m$  then  $d\sigma/dq^2 d\nu$  is independent of  $E$ .

The derivation here is exactly analagous to that which holds to the prediction of the energy independence of the elastic or  $N^{*++}$  production cross sections. Neither scale invariance, nor the non-existence of a vector boson is assumed and thus the method provides a powerful method of determining the spectrum shape which is entirely practical with the numbers of events available in the neon run.

#### V. MUON DETECTION

Muons can be distinguished from hadrons by inserting a large amount of material in the path of the particle, and making use of the fact that the hadrons will undergo strong interactions in the material, but the muons will not. We have considered three possible variations of this technique: a) making use of the liquid neon in the chamber, with no additional material, b) inserting a thick metal plate into

the sensitive region of the chamber, so that particles emerging from the plate are visible in the chamber, and c) placing the hadron absorber external to the chamber, followed by some electronic particle detection system.

In our calculation, we used the interaction length deduced from the experimentally measured interaction cross section of pions in various materials.<sup>9</sup> We define the interaction length as the distance in which a fraction equal to  $(1-1/e)$  of a beam of particles suffers a strong interaction. However, in any particular application, not all of the interactions are detectable; it is therefore relevant to calculate an "effective interaction length" as the distance in which a fraction equal to  $(1-1/e)$  of the beam suffers interactions which can be recognized as such. We find the interaction length in liquid neon, steel, and lead to be 79 cm, 17 cm, and 18.1 cm, respectively. For our application, we estimate the respective effective interaction lengths to be 87 cm, 18.7 cm, and 18.8 cm.

a. Neon only. Figure 13 shows the fraction of pions escaping a detectable interaction in liquid neon, using 87 cm as the effective interaction length. For an average path of 2 m, about 10% of the pions will fake muons. However, if the fiducial volume were restricted to the front half of the chamber, the average path is 3 m and only 3% of the pions will fake muons. As can be seen from Fig. 13, the background remaining after using neon only is too large for the four fermion process or the largest mass W's detectable.

b. Plate inside chamber. After consulting with the group building the chamber, stainless steel was picked as the most desirable material for the plate (the chamber body is stainless steel). Lead is possible, but it would have to be somewhat thicker and more than one and a half times as heavy for the same number of interaction lengths.

The configuration of the plate in the chamber is shown in Fig. 14 . The diameter is 2.6 m, with an average thickness of 85 cm. The plate is tapered slightly so that 3 cameras can see the region in front of the plate; 2 cameras can see behind the plate.

The dashed line on Fig. 14 indicates the  $10 \text{ m}^3$  useful fiducial volume in front of the plate. There is approximately 50 cm of visible region behind the plate. This region can be used to measure the angle and the momentum of tracks emerging from the plate. This is very important in discriminating against hadrons that interact producing a single small angle secondary.

Muons below 1.1 BeV/c momentum will be stopped in the plate. However, these muons will usually not even reach the plate because of their deflection in the chamber magnetic

field. These very low momentum muons, however, will be trapped in the chamber and can be identified by their range. Even above 1.1 BeV/c, some fraction of the particles do not make it through the plate because of the deflection in the magnetic field. A rough estimate of the fraction of the particles that are trapped or go through the plate as a function of momentum is shown in Fig. 15. With this arrangement, we have a sizeable efficiency for muon identification over the entire momentum range.

Averaged over our fiducial volume, 0.4% of the hadrons will transverse the plate without having a detectable interaction in the plate or the neon in front of it. The fraction of the pions that decay before interacting is shown as a function of the pion momentum in Fig. 16. From this figure, we see that generally less than 1% of the pions (hadrons) fake  $\mu$ 's, and the fraction is below 1/2% above 2 1/2 BeV/c.

The cost for the stainless steel plus fabrication has been estimated to be around \$50,000.

c. External Muon Identifier. The feasibility of external muon identifiers has been considered by a number of groups. In order to satisfy the requirements of this experiment, i.e. approaching 99% reliable  $\mu$  identification, at least 6 interaction lengths of material is required, and at least two planes of external particle detectors. The cost for such a system has been estimated to be more than 10 times the cost of the plate, and even then it would have some

disadvantages compared to the plate for this particular experiment.

We summarize some of the advantages and disadvantages of using an internal plate.

Advantages:

- a. Hadron rejection better than 99 1/2% for most momenta (external identifier is at best 95%-98%.)
- b. Has finite geometric efficiency at all momenta (external identifier would not be useful below 4 BeV/c, which is a very useful region in this experiment).
- c. Plate is relatively inexpensive.
- d. Simplicity of operation during run.
- e. More reliable correlation of tracks before and after plate (with external detector, particles pass through coils and fringe field of the chamber, and it is not clear how reliable the correlation will be).
- f. Muon identification can be made on the scan table. Thus, reducing greatly the number of events to be measured to find the muon pair events.

Disadvantages of Plate:

- a. Cuts the useful fiducial volume of the chamber by a factor of two.
- b. Hurts momentum measuring precision on moderate energy tracks. For the high energy muons traversing the plate, however, the coulomb scattering in the plate is negligible compared to the measuring errors, and the full length of the track before and after the plate can be used.
- c. Logistics of inserting and removing the plate.
- d. 5 cameras are required instead of 3.

## REFERENCES

- 1 T.D. Lee, Phys. Rev. Letters 25, 1144 (1970).
- 2 R.W. Brown, J. Smith, Phys. Rev. D3, 207 (1971).
- 3 We would like to thank Prof. T.D. Lee and Dr. W.A. Cooper for their help in calculating the cross sections for the scalar boson production process.
- 4 W. Czyz, G.D. Sheppy, J.D. Walecka, Il Nuovo Cimento 34, 404 (1964).
- 5 D. Carey, Y. Kang, F. Nezrick, R. Stefanski, J. Walker, NAL Report TM-265; F. Nezrick, Y. Kang, private communication.
- 6 We would like to thank Dr. K. Fujikawa of Princeton University for making these results available to us.
- 7 J. Loveseth, M. Radomski, Phys. Rev. D3, 2686 (1971).
- 8 The cross sections for single pion production processes by neutrinos have been calculated by Adler, Annals of Physics 50, 189 (1968), using a value of 0.71 for  $M_A^2$ , the axial vector form factor mass squared:
- $$\sigma(\nu n \rightarrow \mu^- n \pi^+) = 0.12 \times 10^{-38} \text{ cm}^2/\text{nucleon}$$
- $$\sigma(\nu n \rightarrow \mu^- p \pi^0) = 0.16 \times 10^{-38} \text{ cm}^2/\text{nucleon}$$
- $$\sigma(\nu p \rightarrow \mu^- p \pi^+) = 0.44 \times 10^{-38} \text{ cm}^2/\text{nucleon} .$$
- In view of the higher cross section obtained for the third of the three reactions in the CERN neutrino experiment, we have assumed the cross sections for all three processes to be twice the calculated value.
- 9 G. Cocconi, Proceedings of the 1960 Rochester Conference on High Energy Physics, p. 804.

TABLE I

 $\nu$  Event Rates in Neon

Total number of events produced in a fiducial volume of  $10 \text{ m}^3$  of neon in  $10^6$  pulses with  $2 \times 10^{13}$  protons on target per pulse, Wideband beam.

<u>Reaction</u>	<u>Primary Proton Energy</u>		
	<u>200 BeV</u>	<u>350 BeV</u>	<u>500 BeV</u>
Total Inelastic	$1.4 \times 10^6$	$3.2 \times 10^6$	$6 \times 10^6$
Elastic	$4.1 \times 10^4$	$6.6 \times 10^4$	$9.6 \times 10^4$
$W_1$ Production			
$m_W = 3 \text{ BeV}$	$2.1 \times 10^5$	$7.9 \times 10^5$	$2.1 \times 10^6$
5	$1.6 \times 10^4$	$9.0 \times 10^4$	$2.8 \times 10^5$
8	720	$8.7 \times 10^3$	$2.3 \times 10^4$
10	60	$1.6 \times 10^3$	$8.7 \times 10^3$
15	-	6	160
$W_0$ Production			
$m_0/m_1 = 2.5/5 \text{ BeV}$	$1.0 \times 10^3$	$3.6 \times 10^3$	$9.5 \times 10^3$
5/10	5	61	257
7.5/15	-	5	23
$\nu + \text{Ne} \rightarrow \text{Ne} + \mu^- + \mu^+ + \nu$	8	20	50
$\nu + \text{Ne} \rightarrow \text{Ne} + \mu^- + \tau^+ + \nu$	18	44	104

## FIGURES

1. Cross Sections
2.  $W_0$  Cross Section
3.  $\nu$  Fluxes
4.  $W_1$  Production
5.  $W_0$  Production
6. Four Fermion vs  $E_\nu$
7. Total Inelastic vs  $E_\nu$
8. Angle and Momentum of  $\pi^+$  from CERN Events
9. Angular Distribution of 4 Fermion Events
10.  $P_L$  for W and Background
11. W Search In Total Cross Section
12. Background with and without Plate
13. Fraction of  $\pi$ 's Escaping Detection
14. Plate in Chamber
15. Plate efficiency vs P
16. Fraction of  $\pi$  Faking  $\mu$ 's
17. Double Plate



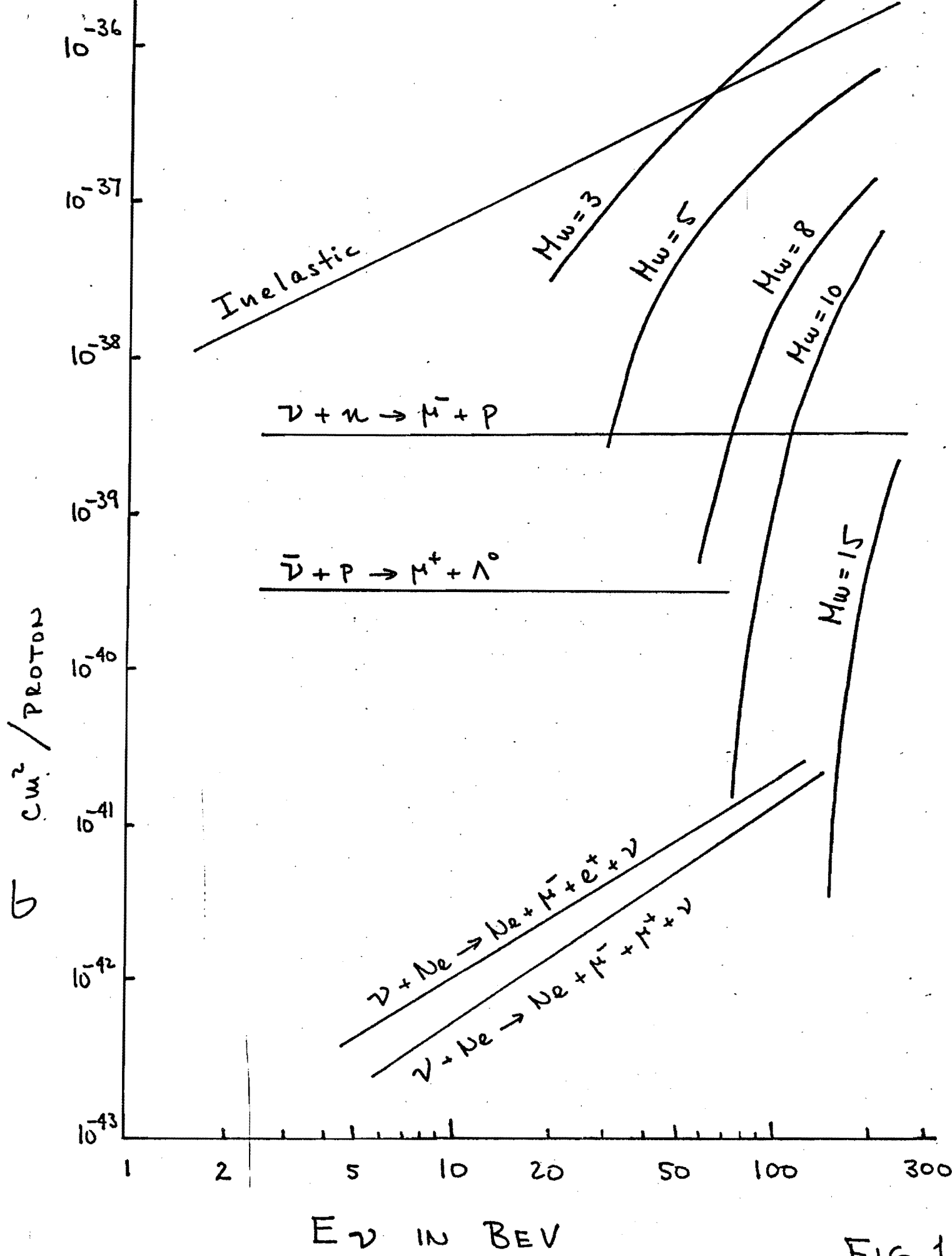


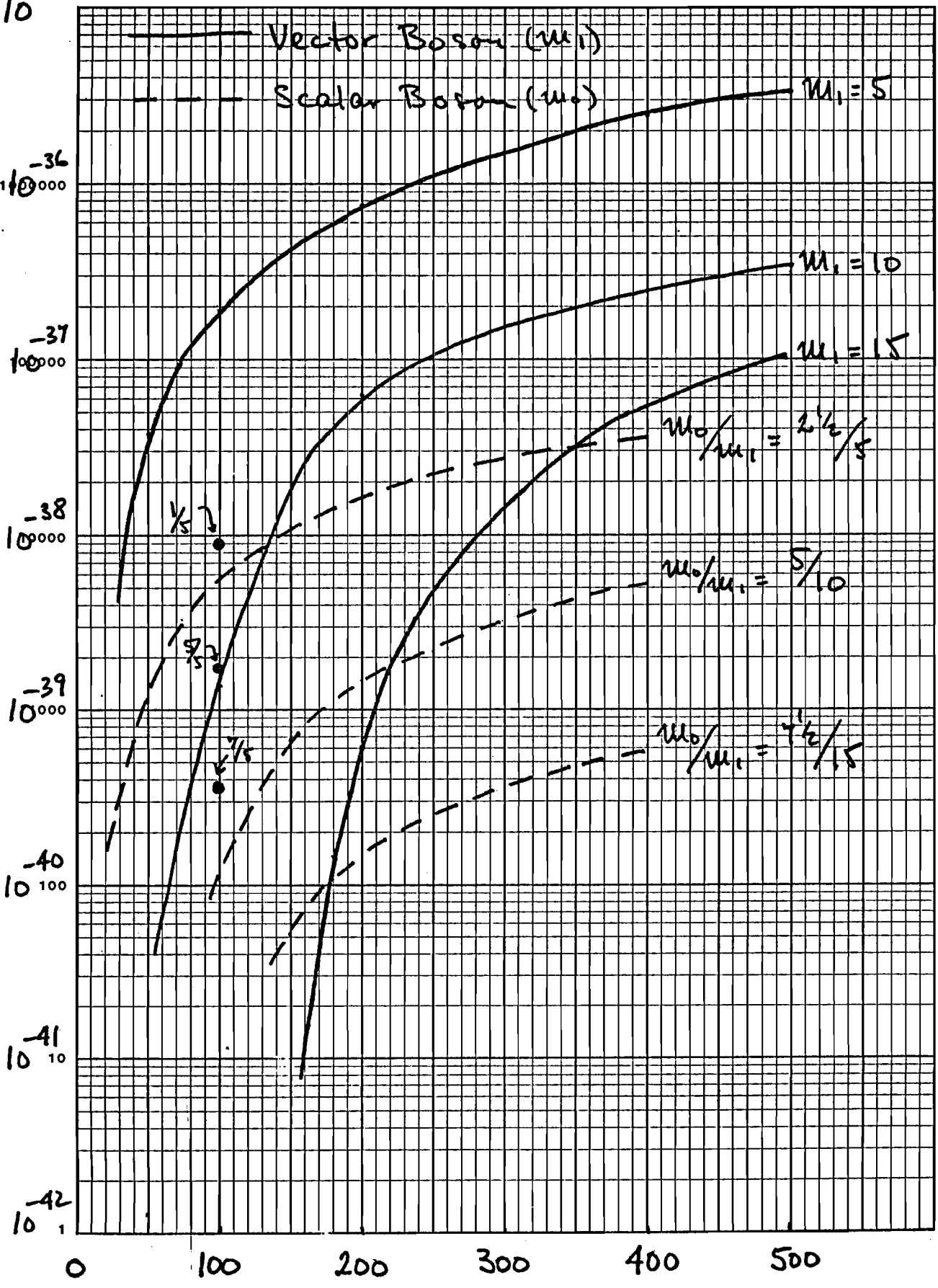
FIG 1

$\nu + \text{Ne} \rightarrow \text{Ne} + \mu^- + W^+$  Production Crosssections

$10^{-35}$  MODEL

DATE

$\sigma$  (cm<sup>2</sup>/proton)



SEMI-LOGARITHMIC 359-96  
 KEUFFEL & ESSER CO. MADE IN U.S.A.  
 7 CYCLES X 80 DIVISIONS

$E_\nu$  in BeV

FIG 2

# V SPECTRA

Horn Focused Beam

400 m Decay Path

1000 m Shield Length

$\nu / \text{Bev} / \text{m}^2 / 10^{13} \text{ int. prot.}$

SEMI-LOGARITHMIC 46 6212  
5 CYCLES X 70 DIVISIONS  
KEUFFEL & ESSER CO.

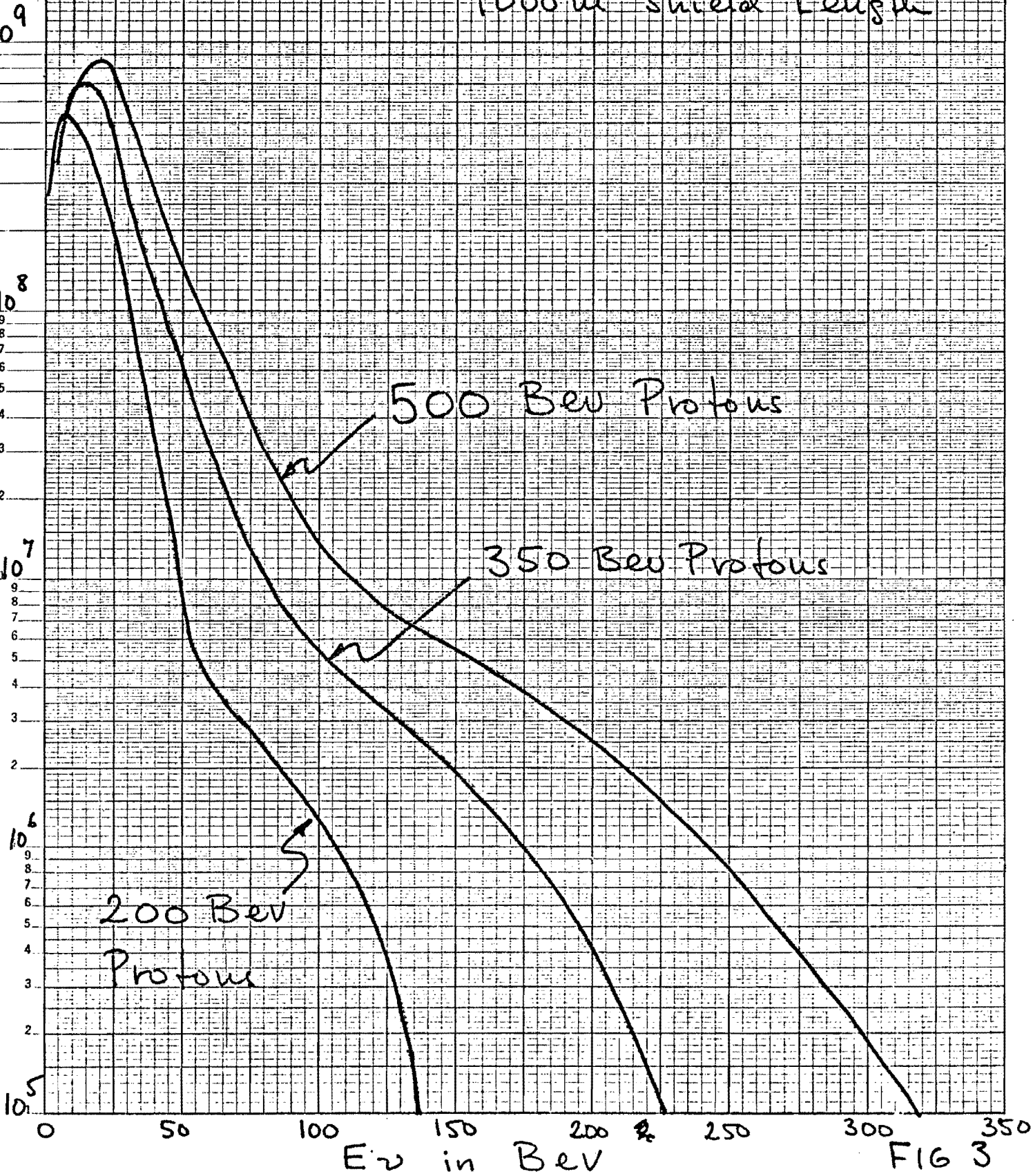
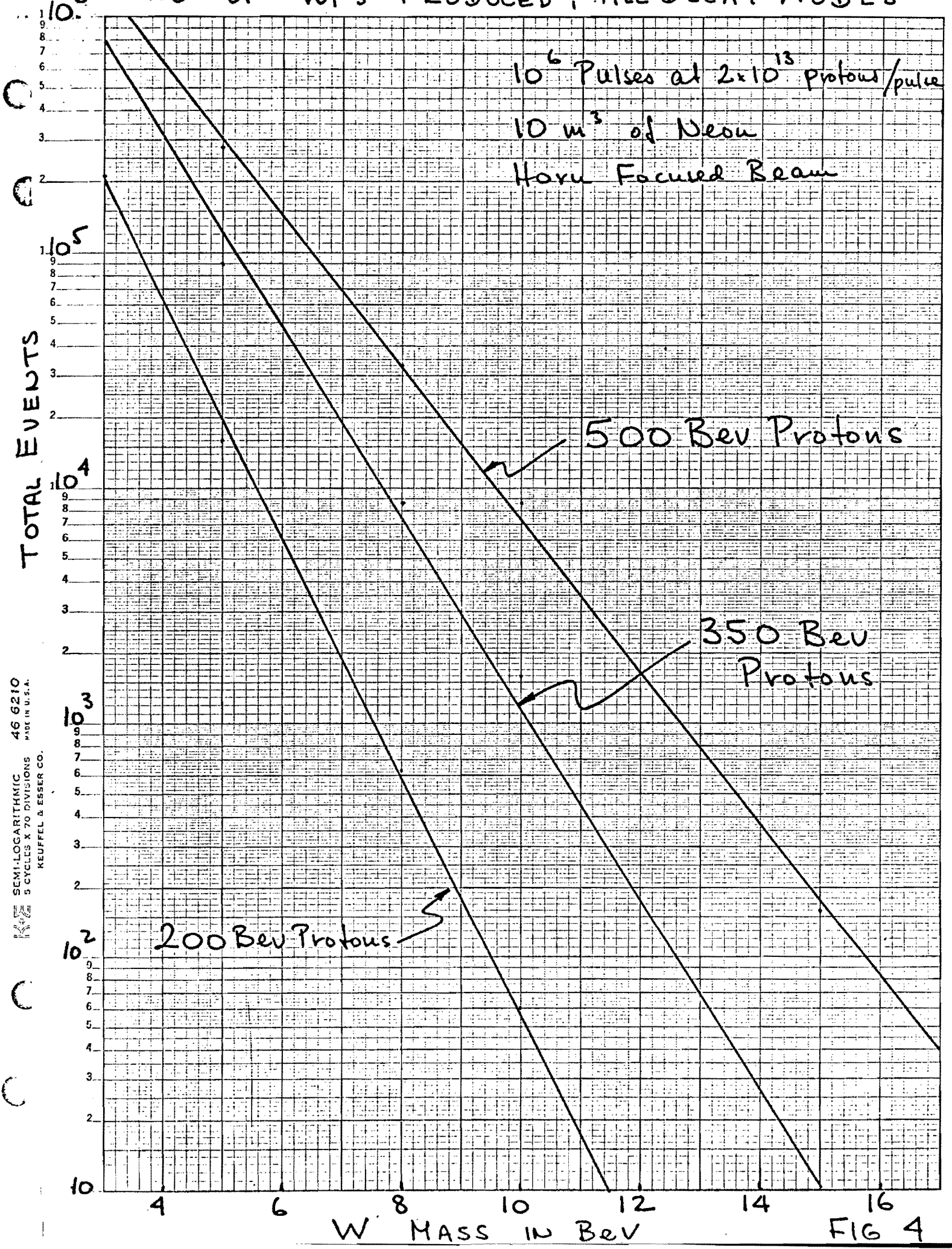


FIG 3

NO. OF WIS PRODUCED, ALL DECAY MODES



SEMI-LOGARITHMIC 46 6210  
5 CYCLES X 70 DIVISIONS MADE IN U.S.A.  
KEUFFEL & ESSER CO.

FIG 4

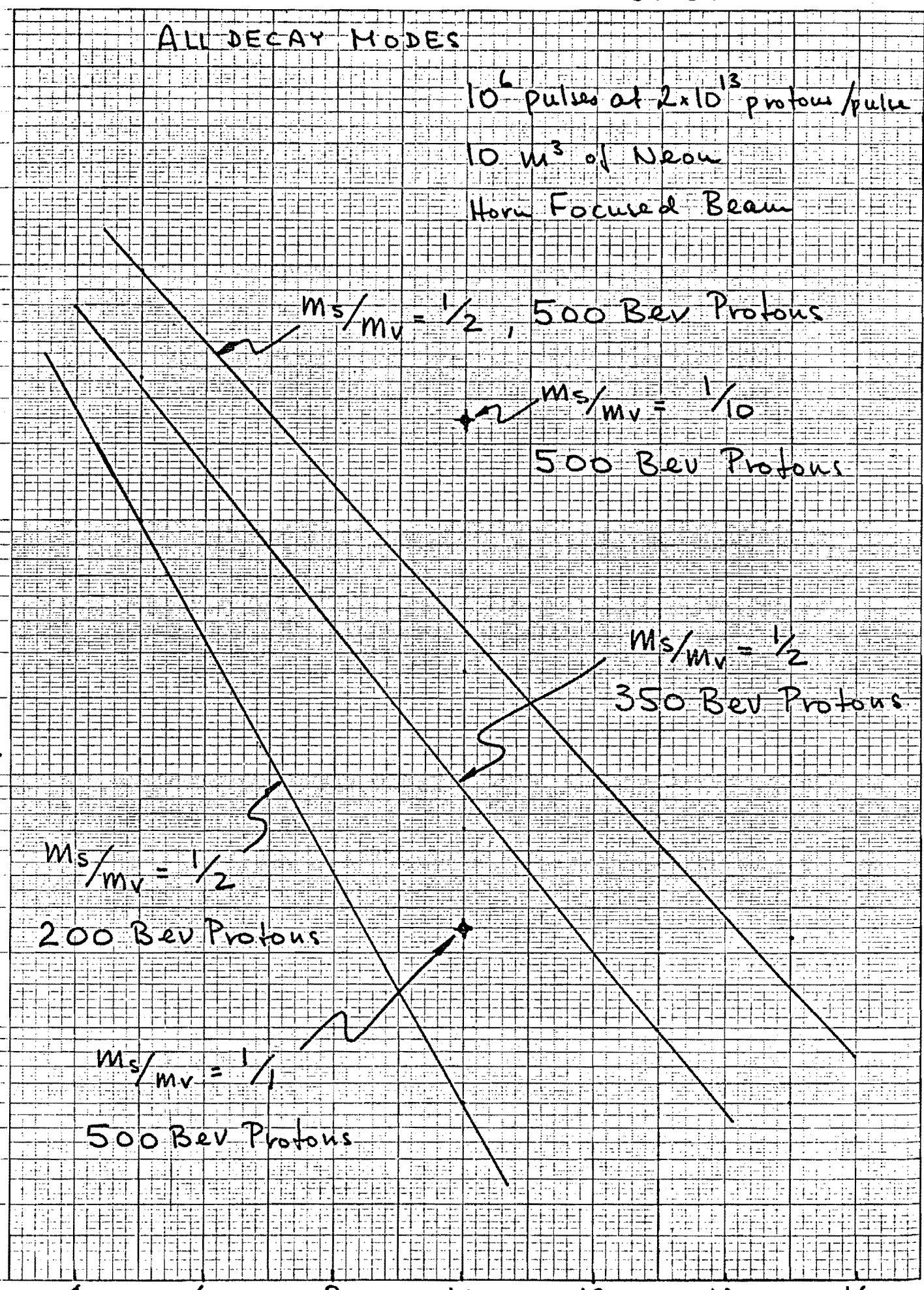
NUMBER OF SCHLAK BOSONS PRODUCED

ALL DECAY MODES

$10^6$  pulses at  $2 \times 10^{13}$  protons/pulse  
 10 m<sup>3</sup> of Neon  
 Horn Focused Beam

TOTAL EVENTS

SEMI-LOGARITHMIC 46 6210  
 5 CYCLES X 70 DIVISIONS MADE IN U.S.A.  
 KEUFFEL & ESSER CO.



$m_s/m_v = 1/2$ , 500 BeV Protons

$m_s/m_v = 1/10$   
 500 BeV Protons

$m_s/m_v = 1/2$   
 350 BeV Protons

$m_s/m_v = 1/2$   
 200 BeV Protons

$m_s/m_v = 1/1$   
 500 BeV Protons

MASS OF VECTOR BOSON IN BEV

FIG 5



46 6210  
MADE IN U.S.A.  
5 CYCLES X 70 DIVISIONS  
KUFFEL & ESSER CO.

EVENTS / 10 BeV

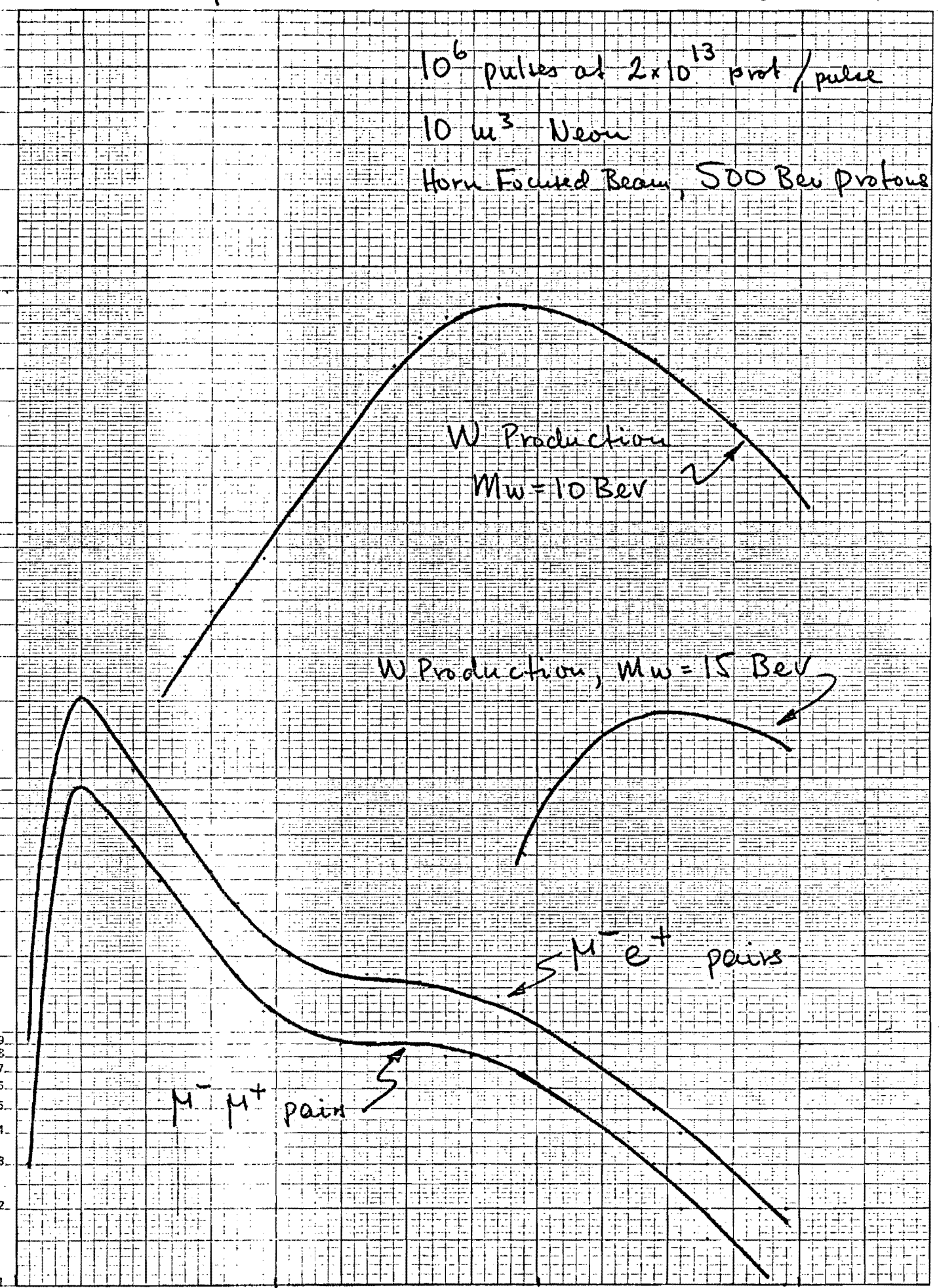
$10^6$  pulses at  $2 \times 10^{13}$  prot / pulse  
 $10 \mu^3$  Neon  
Horn Focused Beam, 500 BeV protons

1000

100

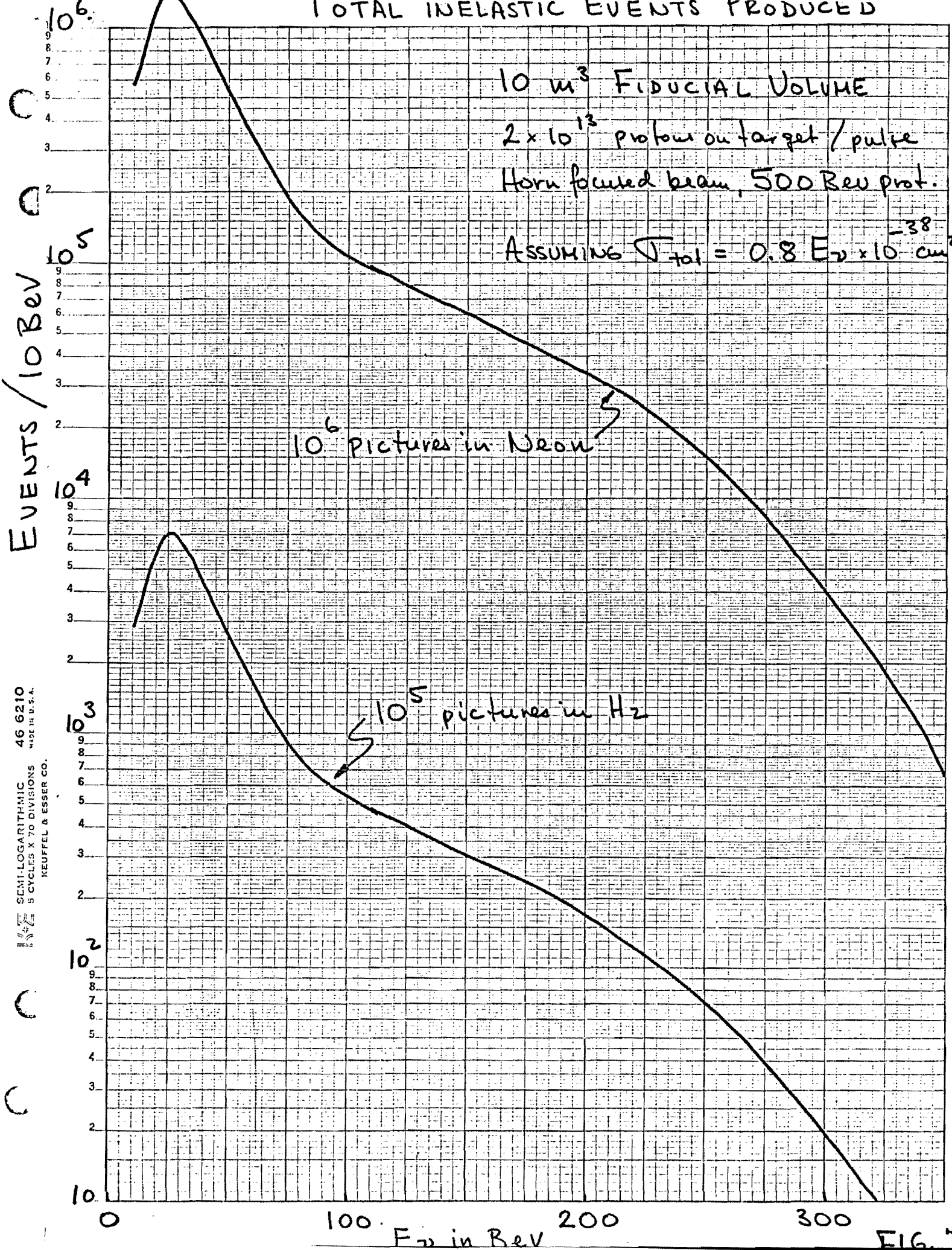
10

1



0 100 200 300  $E_\nu$  in BeV FIG 6

# TOTAL INELASTIC EVENTS PRODUCED

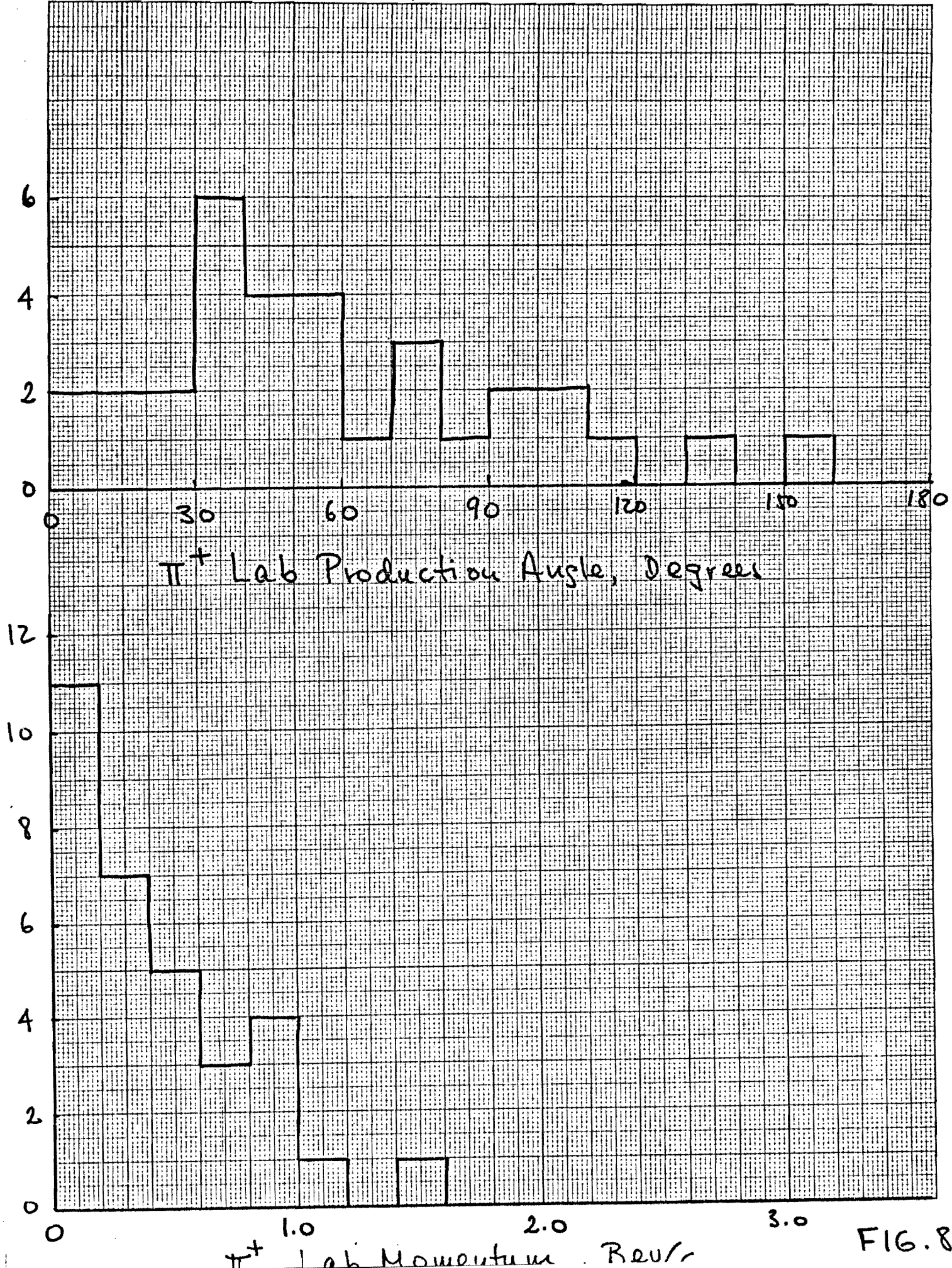


KEUFEEL & ESSER CO.  
 5 CYCLES X 70 DIVISIONS  
 MADE IN U.S.A.  
 46 6210  
 SEMI-LOGARITHMIC

FIG. 7



32 CERN EVENTS



EUGENE DIETZGEN CO. MADE IN U. S. A. MILLIGRAM DRAFT PAPER MILLIMETER

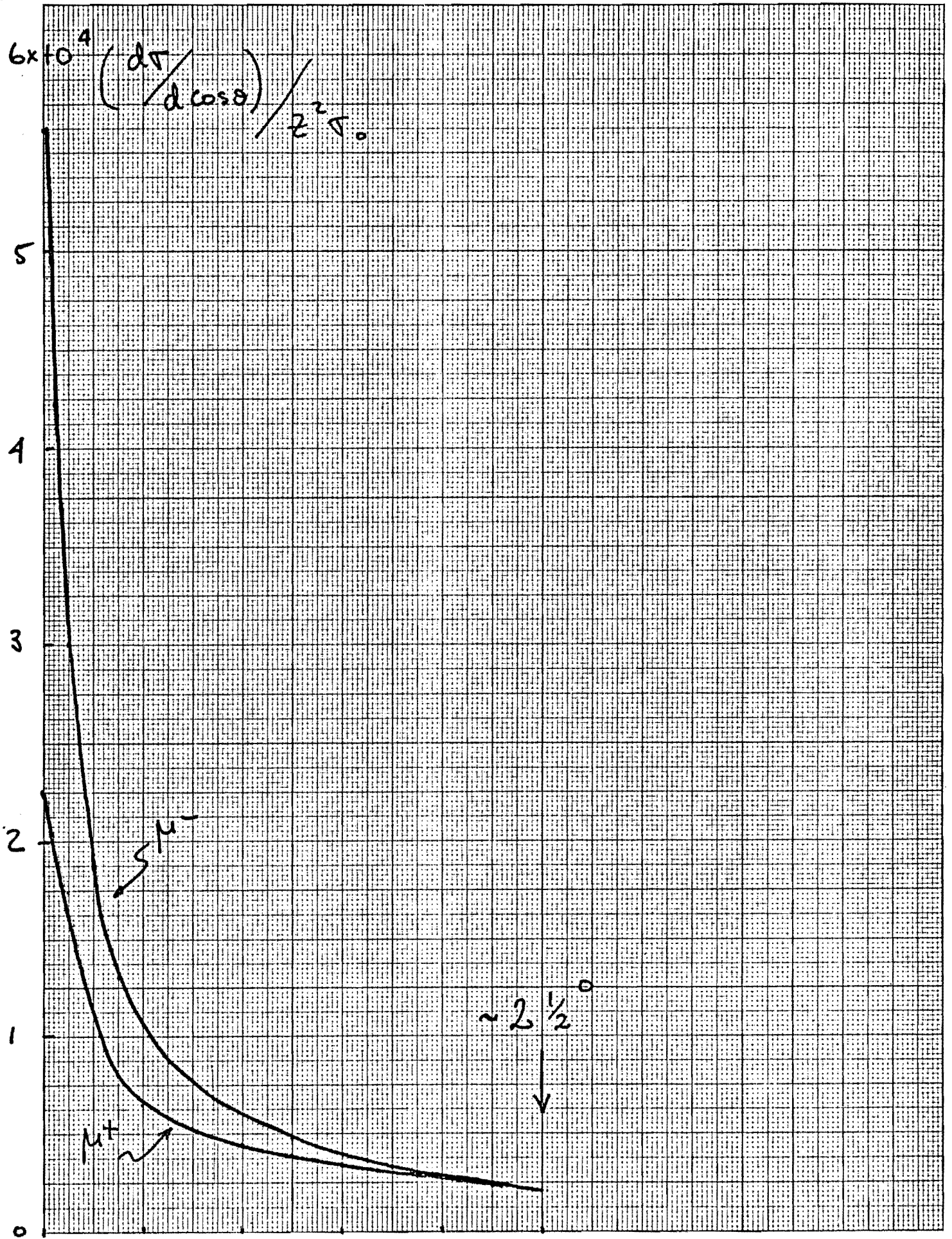
FIG. 8



$$\nu + \bar{\epsilon} \rightarrow \bar{\epsilon} + \mu + \mu + \nu$$

at  $E\nu \text{ inc.} = 40 \text{ keV}$

EUGENE DIETZGEN CO. MADE IN U. S. A. NO. 341-M DIETZGEN GRAPH PAPER MILLIMETER



1.0 .9998 .9996 .9994 .9992 .9990  
 $\cos \theta$  of  $\mu$  in Lab

FIG. 89

# TRANSVERSE MOMENTUM DISTRIBUTION OF $\mu^+$ FROM $W^+$ DECAY & BACKGROUND.

EVENTS / 0.5 Bev/c  $P_T$

SEMI-LOGARITHMIC 46 6210  
5 CYCLES X 70 DIVISIONS MADE IN U.S.A.  
KEUFFEL & ESSER CO.

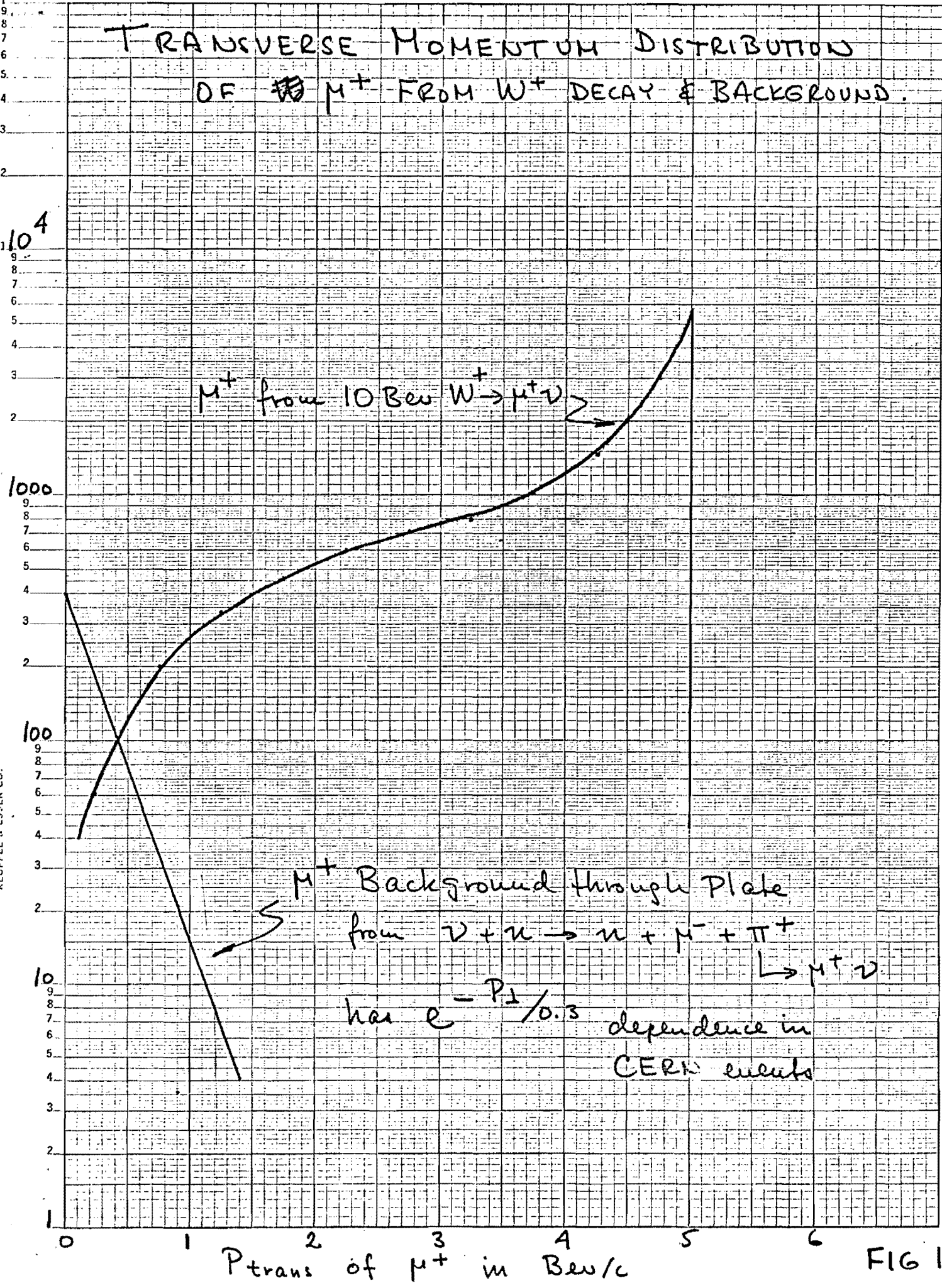


FIG 10

# TOTAL CROSSSECTION VS. $E_\nu$



FOR  $W$  MASSES OF 10, 20 & 37 BeV.

$\sigma_{\text{tot}}$

$2.4 \times 10^{-36} \text{ cm}^2$

$M_W = \infty$

37.29

20

10 BeV

$E_\nu$  in BeV

FIG 11

EUGENE DIETZGEN CO.  
MADE IN U. S. A.

NO. 341-M DIETZGEN GRAPH PAPER  
MILLIMETER

0 100 200 300

1.6

0.8

0



EVENTS /  $2 \times 10^{11}$  PROTONS

46 6210  
SEMI-LOGARITHMIC  
5 CYCLES X 70 DIVISIONS  
KEUFFEL & ESSER CO.

$10^6$  Pulses at  $2 \times 10^{13}$  prot/pulse  
 $10 \text{ m}^3$  of Neon  
Horn Focused Beam  
500 BeV Protons

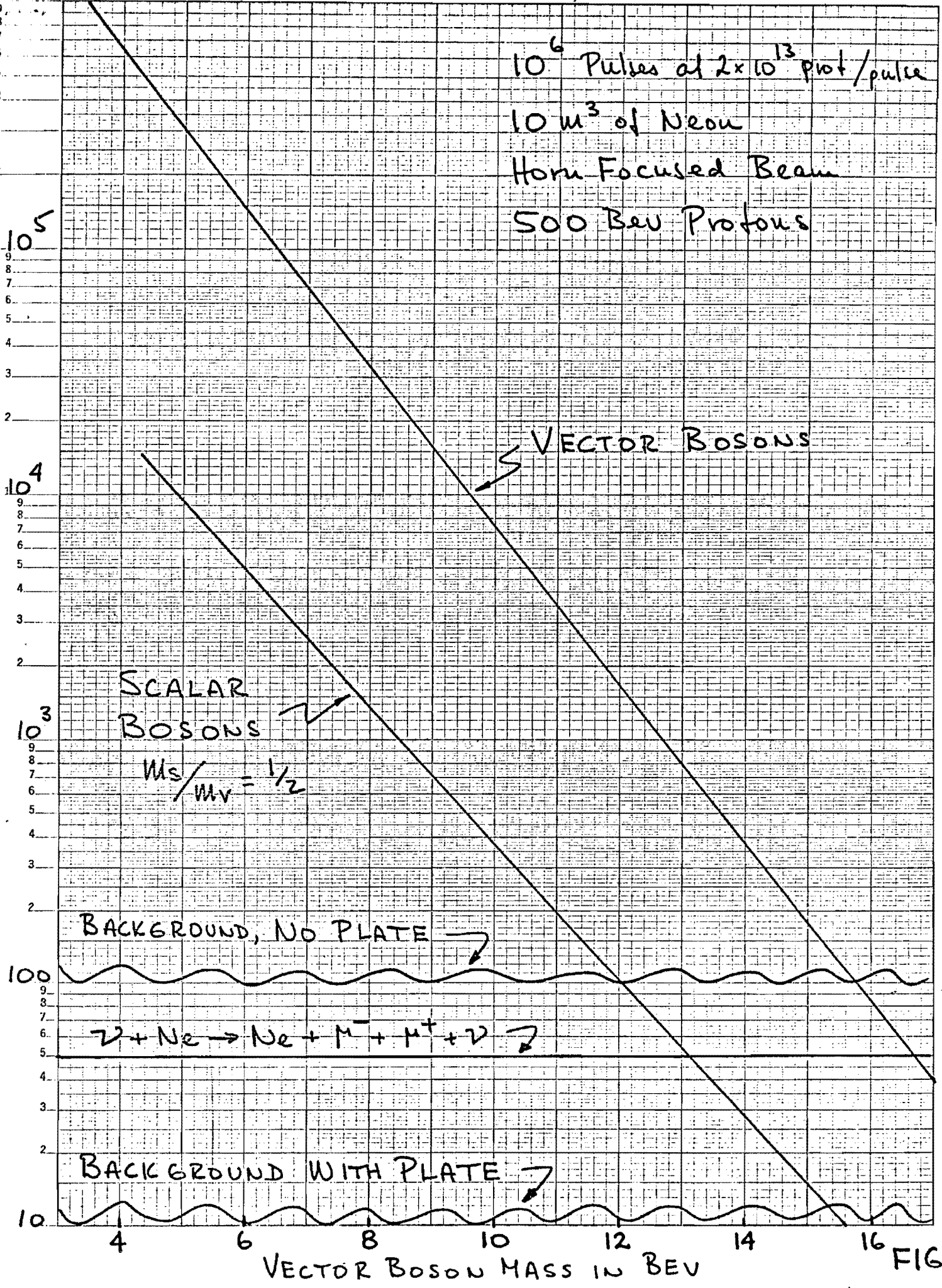
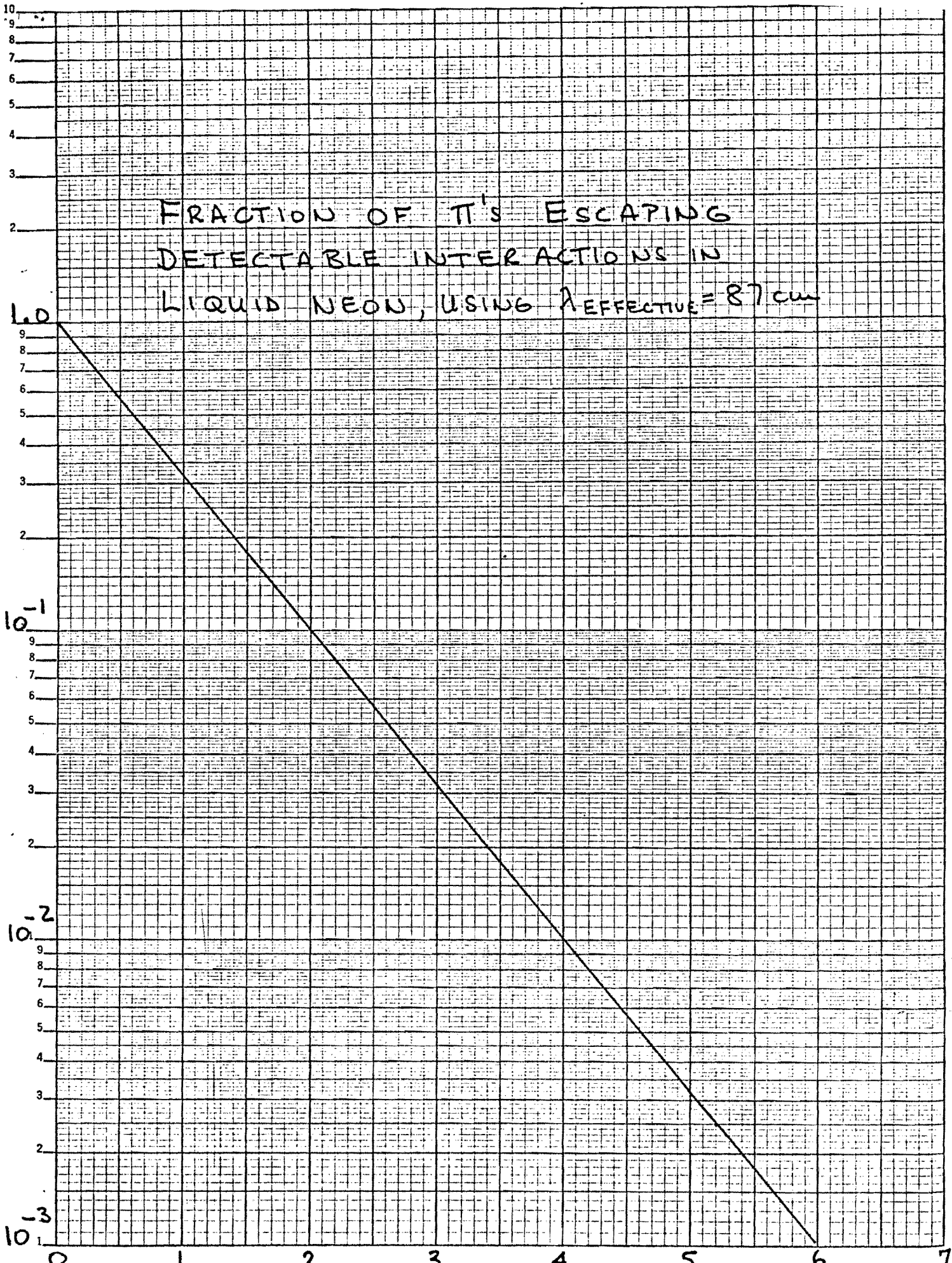


FIG 12

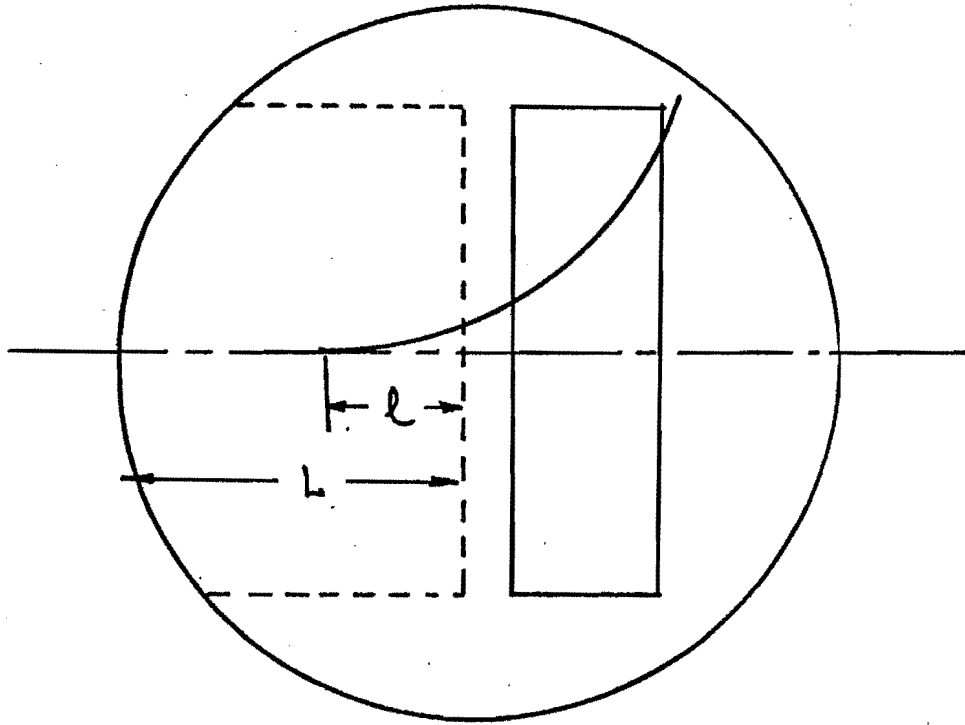
45 6012  
SEMILOGARITHMIC  
5 CYCLES X 70 DIVISIONS  
KEUFFEL & ESSER CO.



FRACTION OF  $\pi$ 'S ESCAPING  
DETECTABLE INTERACTIONS IN  
LIQUID NEON, USING  $\lambda_{EFFECTIVE} = 87 \text{ cm}$

PATH IN NEON IN METERS

FIG 13



$$\text{FRACT} = \frac{l}{L}$$

$l/L$  IS A ROUGH ESTIMATE OF THE GEOMETRIC EFFICIENCY FOR  $\mu$ -HADRON DISCRIMINATION

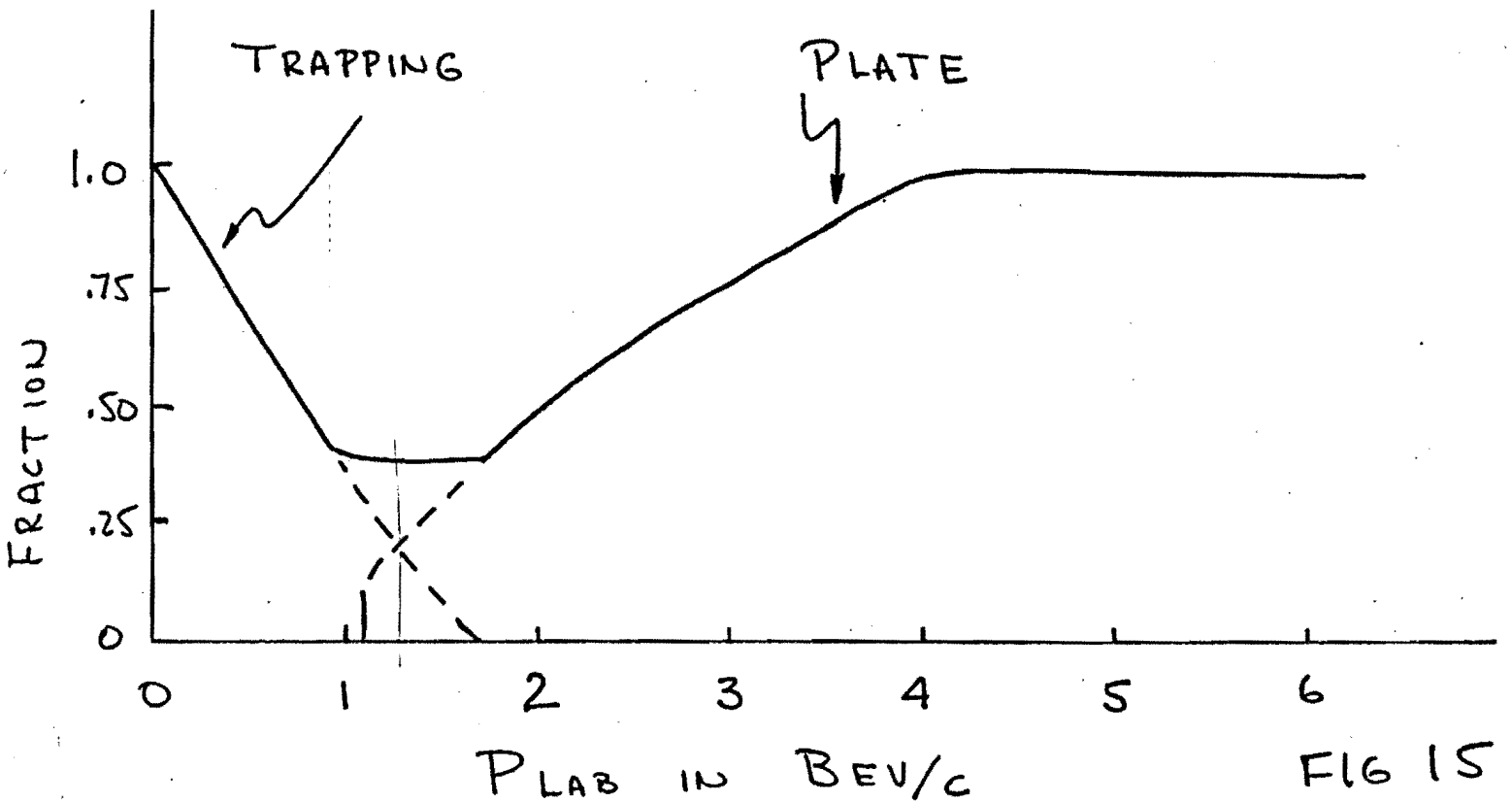


FIG 15

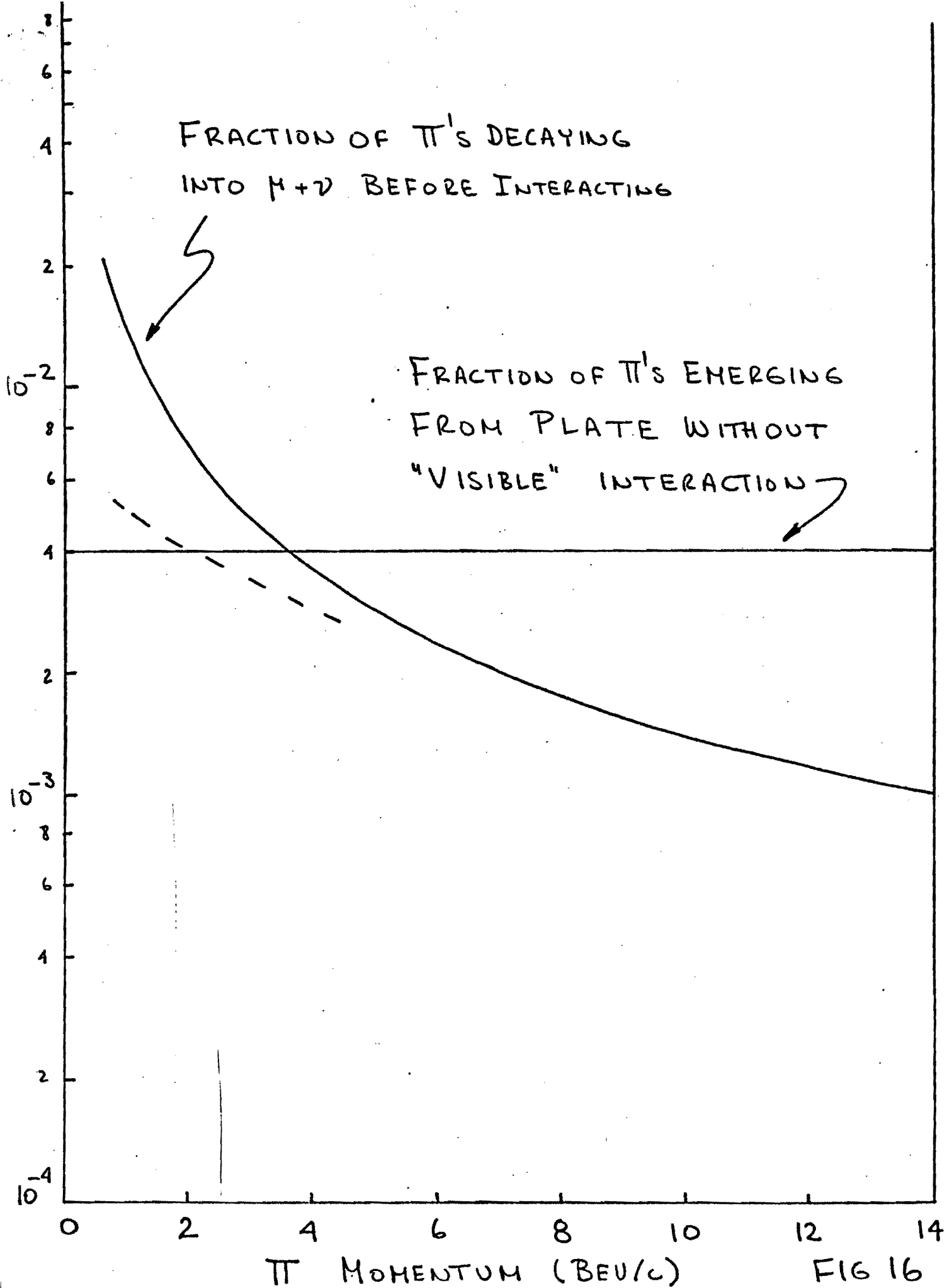


FIG 16

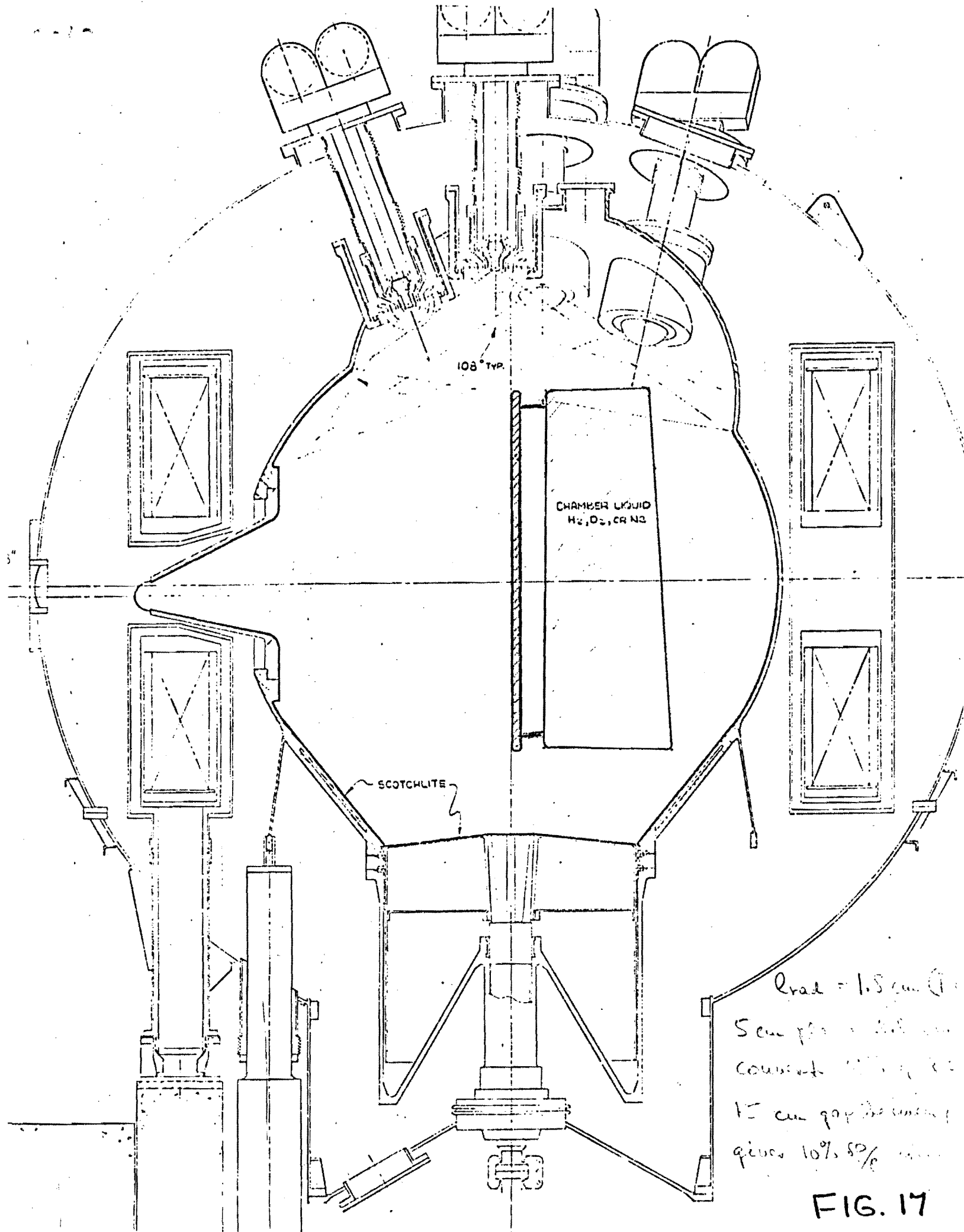


FIG. 17